

UNIVERSITY OF GONDAR
POSTGRADUATE PROGRAMME
COLLEGE OF NATURAL AND COMPUTATIONAL SCIENCE
DEPARTMENT OF CHEMISTRY



Sustainable Green Synthesis of Gold Nanoparticles, Characterization and Its Antibacterial Activities Using Olibanum Gum Of Boswellia Papyrifera.

BY:

Ayal Adugna Mesfin

ADVISOR: - DR. Alle Madhusudhan

June, 2015

Gondar, Ethiopia

Sustainable Green Synthesis of Gold Nanoparticles, Characterization and Its
Antibacterial Activities Using Olibanum Gum of *Boswellia Papyrifera*.

Ayal Adugna Mesfin

A Thesis Submitted to Department of Chemistry, School of
Graduate Studies, University of Gondar

In Partial Fulfillment of Requirements for the Degree of
Master of Science in Chemistry (Analytical Chemistry).

University of Gondar

Gondar, Ethiopia

June, 2015

DECLARATION

First I declare that this thesis is my original work and that all sources of materials used for this thesis have been dully acknowledged. This thesis has been submitted in partial fulfillment of the requirements for M.Sc. degree at University of Gondar and is deposited at the University library to be made available to borrow under rules of library. I solemnly declared that this thesis is not submitted to any other institution anywhere for the award of any academic degree, diploma, or certificate.

Brief quotation from this thesis is allowed without special permission provided that accurate acknowledgement of source is made. Requests for permission for extended quotation from or reproduction of this manuscript in whole or in part may be granted by the Head of Chemistry department when in his or her judgment the proposed use of the material is in the interest of scholarship. In all other instances, however, permission must be obtained from the author.

Name: Ayal Adugna Mesfin

Signature _____

Place: University of Gondar

Date of submission: _____

UNIVERSITY OF GONDAR
POSTGRADUATE PROGRAMME

This is certify that this thesis prepared by **Ayal Adugna Mesfin** entitled “*Sustainable Green Synthesis of Gold Nanoparticles, Characterization and Its Antibacterial Activities Using Olibanum Gum of Boswellia Papyrifera*” has been submitted for examination with my approval as university advisor and submitted and approved for the degree of masters of science in chemistry complies with the regulation and meets the accepted standards with respect to originality and quality.

Boards of examiners

Approved by

Thesis supervisor/Advisor

Signature

1. Dr. Alle Madhusudhan
Research Advisor

2. _____

Chair Person

3. _____
Examiner

4. _____

Examiner

ACKNOWLEDGMENT

I would like to express my sincere gratitude to my research advisor Dr. Alle Madhusudha for his full guidance, timely advice, incessant support, inspiration and giving me very helpful comments, valuable suggestions throughout my thesis work. He is such an energetic and knowledge intellectual that he helped me in conceiving a new idea and designing the work. I would also like to appreciate his utmost effort and patience in following up this work from the very beginning to the end with unreserved support for the characterization of the data; for his fatherly advice in all aspect and achievements of today's success.

I would also like to acknowledge the encouragement I received from Mr. Mulugeta Legesse, a member of the University of Gondar, department of chemistry for his deep knowledge and positive support while the practical work was run. I am also grateful to Mr. Tadie, a staff member of department of biotechnology for all support extended to me while the antibacterial activity of the synthesized AuNPs has been done on their laboratory.

Special thanks go to staff members of chemistry department for their positive outlook towards encouraging me starting from the conception of the proposal to the materialization of this thesis work. In this connection, laboratory assistants should also deserve special thanks for their supportive help in searching chemicals, reagents and lab equipments.

I also want to thank to Mr. Atnafu Guadie and my all families who always inspire me to make change in my academic performance. Specially, I want to thanks my father for his courage and perseverance which has been an inspiration to me and I dedicate this thesis to him.

Finally department of chemistry, University of Gondar is strongly acknowledged for all the chemicals and lab-equipments it presented for the completion of the work.

Above all, this is my right time to present thanks to omniscient God for all the things he has done in my life, I have no words which help me to express my praise to him, let me keep silent otherwise.

TABLE OF CONTENTS

Contents

ACKNOWLEDGMENT.....	v
TABLE OF CONTENTS.....	vi
LIST OF FIGURES.....	viii
LIST OF ABBREVIATION	ix
ABSTRACT.....	x
1. INTRODUCTION	1
1.1. General features of Gold Nanoparticles (AuNPs).....	4
1.1.1. Localized surface Plasmon resonance	4
1.1.2. Biocompatibility	4
1.1.3. Chemical stability.....	5
1.2. Types of Gold Nanoparticles.....	6
1.3. Synthesis of Gold Nanoparticles.....	7
1.4. The olibanum gum of <i>Boswellia papyrifera</i>	10
1.4.1. Description of the genus.....	10
1.5. Objectives	13
1.5.1. The general objective.....	13
1.5.2. The specific objectives	13
2. REVIEW OF LITERATURE.....	14
3. SCOPE OF THE PRESENT STUDY	19
4. MATERIALS AND METHODS	20
4.1. Synthesis of AuNPs.....	20
4.2. Characterization.....	21
4.2.1. UV–Visible spectra	21
4.2.2. FTIR spectra.....	21
4.2.3. XRD analysis	21
4.2.4. TEM analysis.....	22
4.2.5. Antibacterial property of AuNPs	22
5. RESULTS AND DISCUSSION.....	23
5.1. Uv-Visible spectra	23
5.2. FTIR analysis of AuNPs	24

5.3. XRD analysis of AuNPs.....	24
5.4. TEM Analysis of AuNPs.....	25
5.5. Stability study	26
5.6. Microbial Activity.....	27
6. CONCLUSION.....	29
7. REFERENCES	30
APPENDICES	37

LIST OF FIGURES

Figure 1. A <i>B. papyrifera</i> tree (centre), its flowers (upper left), leaves (right), bark with a frankincense tear (lower left) and flaking bark (centre bottom)	10
Figure 2 . The distribution of <i>B. papyrifera</i> (Del.) Hochst in Africa	11
Figure 3. Gum (Frankincense) of <i>B. papyrifera</i> after tapping from the plant and sun dried...	11
Figure 4. Tapped, dried Powder gum (Frankincense) of <i>B. papyrifera</i>	12
Figure 5. The UV–Vis absorption spectra of AuNPs synthesized by autoclaving different concentrations of HAuCl ₄ with 0.5 % olibanum gum solution	34
Figure 6. The UV–Vis absorption spectra of AuNPs synthesized by autoclaving different concentrations of olibanum gum solution with 1 mM HAuCl ₄	35
Figure 7. The UV–Vis absorption spectra of synthesized AuNPs by olibanum gum solution with 1 mM HAuCl ₄ 0.5 % of Olibanum gum solution with different autoclave time	36
Figure 8. FTIR spectra of (a) olibanum gum (b) AuNPs capped in olibanum gum	37
Figure 9. XRD pattern of AuNPs stabilized in olibanum gum. Conditions: 0.5 % (w/v) of gum solution, 1 mM of HAuCl ₄ and autoclaved for 15 min at 15 psi.....	38
Figure 10. TEM image of gold nanoparticles synthesized with 1 % (w/v) olibanum gum and 1 mM HAuCl ₄ , autoclaved for 15 min at 15 psi (B) histogram showing the particle size distribution of AuNPs (C) The selected area electron diffraction pattern of the AuNPs.....	39
Figure 11. A. Stability of gold nanoparticles synthesized with 1 % (w/v) olibanum gum and 1 mM HAuCl ₄ , autoclaved for 15 min at 15 psi in different pH condition (pH 2-12) ...	40
Figure 11B. Stability of gold nanoparticles synthesized with 1 % (w/v) olibanum gum and 1 mM HAuCl ₄ , autoclaved for 15 min at 15 psi in different electrolyte condition (10 ⁻¹ to 10 ⁻⁶)....	40
Figure 11C. Stability of gold nanoparticles synthesized with 1 % (w/v) olibanum gum and 1 mM HAuCl ₄ , autoclaved for 15 min at 15 psi in different days (7 to 1 month)	41
Figure 12. Antibacterial activity of AuNPs against <i>S. aureus</i> and <i>E. coli</i> after 24 h of incubation. 1. 5 µL of AuNPs, 2. 5 µL of ampicillin. 3. 5 µL of pure olibanum gum solution).....	41

LIST OF ABBREVIATION

MRI	Magnetic Resonance Imaging
AuNPs	Gold nanoparticles
SPR	Surface plasmon resonance
EM	Electromagnetic
RA	Reducing agent
CA	Capping agent
NaBH ₄	Sodium borohydride
DMF	Dimethyl formamide
OG	Olibanum gum
DHFA	Dihydroxyfumaric acid
FTIR	Fourier transforms infrared
TEM	Transmission electron microscopy
XRD	X-ray diffraction
SAED	Selected-area electron diffraction
FCC	Face centered cubic crystal
THPAL	Trialanine phosphine
ROS	Reactive oxygen species

ABSTRACT

A completely sustainable green, and economical viable route for the synthesis of AuNPs by autoclave has been developed by using only HAuCl_4 as the precursor and olibanum gum (OG) of (*Boswellia papyrifera*) simultaneously as a reducing agent and a capping agent. No extra reagents were needed. From the analyses of UV/Vis absorption spectra, TEM, SAED, and XRD patterns, the formation of AuNPs with fcc structure was recognized. The synthesis reaction was usually finished in 15 mins. Increasing the reaction temperature increased the formation rate but had no significant effect on the optical property and size of AuNPs. With increasing Au (III) ion concentration or gum concentration, the mean diameter of AuNPs slightly has been increased. Also, the particle size distribution became broader at higher Au (III) ion concentration or lower OG concentration due to the insufficient protection. Although raising the gum concentration was helpful to reduce Au (III) ions completely and stabilize the AuNPs, too high gum concentration was not suitable for the stabilization of AuNPs because the increased intermolecular force of gum might hinder the dispersion of AuNPs. Furthermore, the resultant AuNPs were found to remain highly stable in the different pH and NaCl solution. The resulted olibanum gum capped AuNPs were highly stable and had significant antibacterial action on both the *Escherichia coli* (*E. coli*) and *Staphylococcus aureus* (*S. aureus*).

Key Words: AuNPs, Olibanum gum, Synthesis, Characterization, Antibacterial Activity

1. INTRODUCTION

Nanoscience and nanotechnology are recent innovative developments of science and engineering that are evolving at a very fast pace. They are driven by the desire to fabricate materials with novel and improved properties that are likely to impact virtually all areas of physical and chemical sciences, biological sciences, health sciences, and other interdisciplinary fields of science and engineering. The word nano, derived from the Greek nanos, meaning dwarf, is used to describe any material or property which occurs with at least one out of the three dimensions is in 1 to 100 nm are called nanoparticles, whether they are dispersed in gaseous, liquid, or solid media. Nanoparticles are a number of atoms or molecules bonded together (these particles usually contain 10^6 atoms or fewer) and are intermediate in size between individual atoms and aggregates large enough to be called bulk material [1, 2]. Because the nanoparticles are larger than individual atoms and molecules but are smaller than the bulk solid, materials in the nanometer size regime show behavior that is intermediate between that of a macroscopic solid and that of an atomic or molecular system. There are three major factors that are responsible for these differences: high surface-to-volume ratio [2-5], quantum size effect [6] and electrodynamic interactions [7]. Metallic nanoparticles possess unique optical, electronic, chemical, and magnetic properties that are strikingly different from those of the individual atoms as well as their bulk counterparts. Nanometer-scale metal particles exhibit optical properties of great aesthetic, technological, and intellectual value [8]. Colloidal solutions of the noble metals, namely, copper, silver, and gold, show characteristic colors that have received considerable attention from researchers.

Nanoparticles are known to exist in diverse shapes such as spherical, triangular, cubical, pentagonal, rod-shaped, shells, ellipsoidal and so forth. Nanoparticles by themselves or as

building blocks used to construct complex nanostructures such as nanochains, nanowires, nanoclusters and nanoaggregates. These find use in a wide variety of applications in the fields of electronics, chemistry, biotechnology and medicine, just to mention few: For example, gold nanoparticles are being used to enhance electroluminescence and quantum efficiency in organic light emitting diodes [9], palladium and platinum nanoparticles are used as efficient catalysts [10]. Glucose sensors are developed based on silver nanoparticles [11], and iron oxide nanoparticles are used as contrast agents in diagnosing cancer in Magnetic Resonance Imaging (MRI) [12].

Nanoparticles differ from the properties inherent in their bulk counterparts due to large surface to volume ratio. Thus, surface related phenomena/properties are drastically affected with slight modification of size, shape and surrounding media of nanoparticles. Therefore, nanoparticles exhibit electronic, optical, magnetic and chemical properties that are very different from both the bulk and the constituent atoms or molecules.

Nanoparticles are of great interest due to their extremely small size and large surface to volume ratio, which lead to both chemical and physical differences in their properties (*e.g.* mechanical properties, biological and sterical properties, catalytic activity, thermal and electrical conductivity, optical absorption and melting point) compared to bulk of the same chemical composition [13-15]. Therefore, design and production of materials with novel applications can be achieved by controlling shape and size at nanometre scale. Nanoparticles exhibit size and shape-dependent properties which are of interest for applications ranging from biosensing and catalysts to optics, antimicrobial activity, computer transistors, electrometers, chemical sensors, and wireless electronic logic and memory schemes. These particles also have many applications in different fields such as medical imaging, nanocomposites, filters, drug delivery, and

hyperthermia of tumors [16, 17]. There are many important applications for metal nanoparticles in medicine and pharmacy. Gold nanoparticles are among the most common ones used for biomedical applications and in emerging interdisciplinary field of nanobiotechnology.

Gold is the quintessential noble element. By nature, it is highly unreactive and as such, historical artifacts made of gold are able to retain their brilliant luster for thousands of years without tarnishing (i.e. chemical oxidation) or deterioration. In its bulk form, gold's uses in jewelry, coinage, and electronics are well known. Gold thin films commonly present in office windows (only 20 nm thick) are able to transmit large amounts of visible light while efficiently reflecting infrared light ($\lambda > 800$ nm), keeping heat inside in the winter and warm air outside in the summer months [18]. In its molecular form, gold compounds can serve in diverse roles ranging from catalysts [19, 20] to anti-arthritic medications [21].

Gold nanoparticles (AuNPs) have drawn the attention of researchers because of their extensive applications in areas such as biomedical applications and in emerging interdisciplinary field of nanobiotechnology. For instance, oligonucleotide capped AuNPs have been used for polynucleotide or protein detection using various detection/characterization methods, including atomic force microscopy, gel electrophoresis, scanometric assay, surface plasmon resonance imaging, amplified voltammetric detection, chronocoulometry, and Raman spectroscopy [22, 23]. Furthermore, gold nanoparticles have been employed in immunoassay [24], protein assay [25], cancer nanotechnology (especially detection of cancer cells) [26], and capillary electrophoresis [27]. In the field of medicine, gold nanoparticles are used for different proposes. They can be used as markers for biological screening test. After cellular uptake, they can act as precise and powerful heaters (thermal scalpels) to kill cancer [28]. Moreover, gold nanoparticles

are capable of inducing apoptosis in B cell-chronic lymphocytic leukemia (chronic lymphoid leukemia [29].

1.1. General features of Gold Nanoparticles (AuNPs)

The unique combination of a multitude of properties of gold nanoparticles such as biocompatibility, chemical inertness, nontoxic, ease of transport in cellular compartments, and localized surface plasmon resonance makes them excellent candidate for drug delivery, anti-bacterial, anti-fungal treatment.

1.1.1. Localized surface Plasmon resonance

Collective excitation of free electrons in the conduction band of a metal, commonly defined as surface plasmon resonance (SPR), occurs under light irradiation. Noble metal nanostructures such as Au and Ag nanoparticles exhibit size and shaped dependent SPR in the visible range [30]. SPR can result in a localized electromagnetic (EM) field that is significantly higher around the nanoparticle than that of the incident irradiation. For example, the striking colours of metallic nanoparticle solutions (such as gold and silver) are due to the red shift of the plasmon band to visible frequencies, unlike that for bulk metals where the plasmon absorption is in the UV region (Plasmon is a quantum of collective oscillation of free electrons in the metals). This red shift of the plasmon occurs due to the quantum confinement of electrons in the nano particle, since the mean free path of electrons is greater than the nano particle size [31].

1.1.2. Biocompatibility

Biocompatibility is a critical design criterion in the selection of any type of materials, including nanoparticles, for biomedical applications. Many approaches have been developed to

study the biocompatibility. For nanoparticles, the simplest and most effective way to determine the biocompatibility is to first evaluate their cytotoxicity in connection with their size, shape, chemical composition, and specific interactions with cells. Several questions need to be addressed for gold nanoparticles, whether gold nanoparticles can cause adverse effects inside a biological system, how gold nanoparticles are internalized by cells, and subsequently where they localize inside the cells. Although it has been shown that the effect of gold nanoparticles on various types of human cells are size and concentration dependent [32, 33] generally speaking, gold nanoparticles exhibit negligible cytotoxicity over a large range of concentrations [34, 35].

1.1.3. Chemical stability

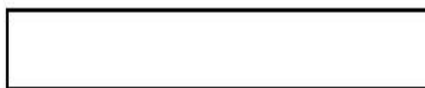
Gold is chemically stable and is resistant to surface oxidation, which is the reason why gold jewellery remains shining even after centuries. These properties together with the high surface to volume ratio determine that gold nanoparticles are important nanomaterials used as reaction platforms or as nanocatalysts in many chemical reactions [36]. It should be noted that other materials such as silver and platinum may have similar catalysis properties, but silver is too reactive to be used and platinum is more expensive than gold [37]. Gold nanoparticles (AuNPs) have attracted great attention because of their stability, oxidation resistance, and biocompatibility. AuNPs have applications in electronics and photonics, catalysis, sensing, imaging, and biomedicine. The size, shape, and crystal structure of AuNPs govern their physicochemical properties along with their catalytic activity. Consequently, synthetic protocols for the production of size- and shape-controlled monodisperse nanoparticles are of paramount importance.

1.2. Types of Gold Nanoparticles

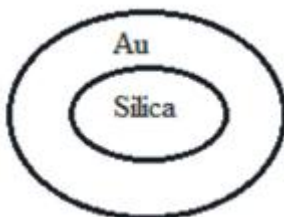
AuNPs generally classified into four types

- Gold nanorods
- Gold nanoshells
- Gold nanocages
- Gold nanosphere

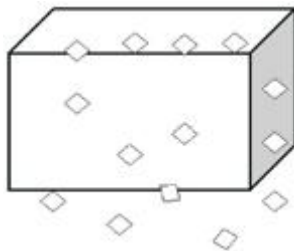
Gold Nanorods: These are synthesized by template method. These are prepared by electrochemical deposition of gold within the pores of nanoporous polycarbonate template membranes. Gold nanorods diameter is according to the diameter of pore of the template membrane



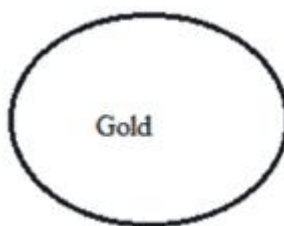
Gold Nanoshells: Surface plasmon resonance peaks (ranging from visible to near I.R. region) is used for the designing and fabrication of gold nanoshells. The core of gold nanoshells is made up of silica and outer surface is made up of gold. Gold controls the thickness of the shell



Gold Nanocage: Through galvanic replacement reaction between truncated silver nanocubes and aqueous HAuCl_4 gold nanocage is synthesized



Solid Nanospheres: These are synthesized by reduction of an aqueous HAuCl_4 using citrate as reducing agent. Through citrates / gold ratio the size of nanospheres can be controlled. By two-phase ratio, the size of nanospheres can be affected by thiol / gold molar ratios



1.3. Synthesis of Gold Nanoparticles

In most cases, AuNPs are synthesized by reducing gold ions with reductants such as borohydride, hydrazine, citrate, etc., followed by surface modification with suitable capping ligands to prevent self-aggregation [38]. In recent years, sol-gel methodology has been utilized to control the nucleation and growth process, thus generating AuNPs of desired size and shape [39]. However, the use of organic solvents in these synthetic processes raises environmental questions [40]. Besides, the conventional approaches often result in the formation of polydisperse nanoparticle populations and require additional separation steps to obtain monodisperse populations [41]. Biosynthetic routes generate negligible quantities of hazardous waste, and consume far less energy than chemical synthesis routes, thereby reducing the AuNPs production cost.

Over the past decade, straightforward, economically viable, and “green” synthesis of nanoparticles has been paid wide attention in the emerging areas of nanoscience and technology [42]. Utilization of cheap and nontoxic chemicals, environmentally benign solvents, and renewable materials are some of pivotal issues in the nanomaterials science field considering “green” synthetic strategy and industrial scale manufacture. It is well known that the reaction medium, reducing agent (RA), and capping agent (CA) are three key factors for the synthesis and stabilization of the metal nanoparticles; these factors should be considered comprehensively from an economic and “green” chemistry perspective.

Most of the synthetic procedures reported to date rely heavily on organic solvents (mainly due to the hydrophobicity of the CA used), thus inevitably resulting in a serious environmental issue while addressing industrial production. So far, some CAs such as thiols and oleic acid have been overwhelmingly utilized to prepare metal and magnetic nanoparticles in organic solvents [43]. Nonetheless, either relatively high cost and toxicity or strict reaction conditions make these CAs less promising in industrial applications. Besides, the strong chemical bonding interaction between the particle surface and capping group not only makes it difficult to separate these CAs from the final products, but also depresses their bacterial activity due to the high surface coverage of the CAs on nanoparticles.

The other concern in the “green” preparation of metal nanoparticles is the choice of RA. The majority of cases so far reported utilize RAs such as hydrazine, sodium borohydride (NaBH_4), and dimethyl formamide (DMF). All of these are highly reactive chemicals and pose potential environmental and biological risks. Although H_2 was also commonly used as RA for the metal nanoparticles synthesis, the difficulty in controlling the amount of H_2 and its combustibility make researchers reluctant to use this gaseous RA. Apparently, a great challenge

being encountered in nanoscience fields is to exploit a straightforward, economically viable, and “green” approach to yield monodisperse metal and semiconductor nanoparticles at ambient temperature and within a short time. Herein, we present a novel and facile approach to rapidly synthesize and effectively stabilize relatively monodisperse AuNPs by employing nontoxic renewable biochemical of olibanum gum (OG) and by autoclaving in the environmentally benign medium of H₂O, which fully adopts the fundamental 12 principles [44] of the “green” chemistry.

Biosynthesis of metal nanoparticles by plants is currently under exploitation. The biological synthesis of gold nanoparticles using plants (inactivated plant tissue, plant extracts and living plant) has received more attention as a suitable alternative to chemical procedures and physical methods. Synthesis of metal nanoparticles using plant extracts is very cost effective, and therefore can be used as an economic and valuable alternative for the large-scale production of metal nanoparticles. Extracts from plants may act both as reducing and capping agents in nanoparticle synthesis. The bio reduction of metal nanoparticles by combinations of biomolecules found in plant extracts (*e.g.* enzymes, proteins, amino acids, vitamins, polysaccharides, and organic acids such as citrates) is environmentally benign, yet chemically complex. Because of the important and critical roles of plants in bio-based protocols for metal nanoparticle production, the green synthesis of metal nanoparticles using plants

In this study, we proposed another environmentally benign process for the synthesis of AuNPs using olibanum gum (OG)) as both the capping and reducing agent without adding extra reducing and capping agent and water as solvent. OG is known as a natural and harmless polysaccharide derived from *Boswellia papyrifera* trees. Due to its well steric stabilization effect as adsorbing on the surfaces of colloids and its numerous functional groups such as carboxylate and amine groups, it has been widely used as emulsifiers and capping agents.

1.4. The olibanum gum of *Boswellia papyrifera*

The dry lands of Ethiopia contain numerous tree and shrub species that produce commercial gums and gum resins. *Boswellia papyrifera* (Del.) Hochst is the most common and economically important one. It is a deciduous multipurpose tree species which is the chief source of commercial product, frankincense or gum olibanum tapped for cash income and local uses in Ethiopia. Frankincense has several traditional uses and a range of industrial applications in pharmacology, cosmetics, detergents, lotions, perfumes, flavouring etc [45-47]. It owns Burseraceae family. It is known for the presence of resin ducts in the bark and production of aromatic oils and resins. The wood is used for pole and timber. The sweet smelling flowers, that appears when the tree fall its leaves, are important sources of nectar for honey bees [48, 49].

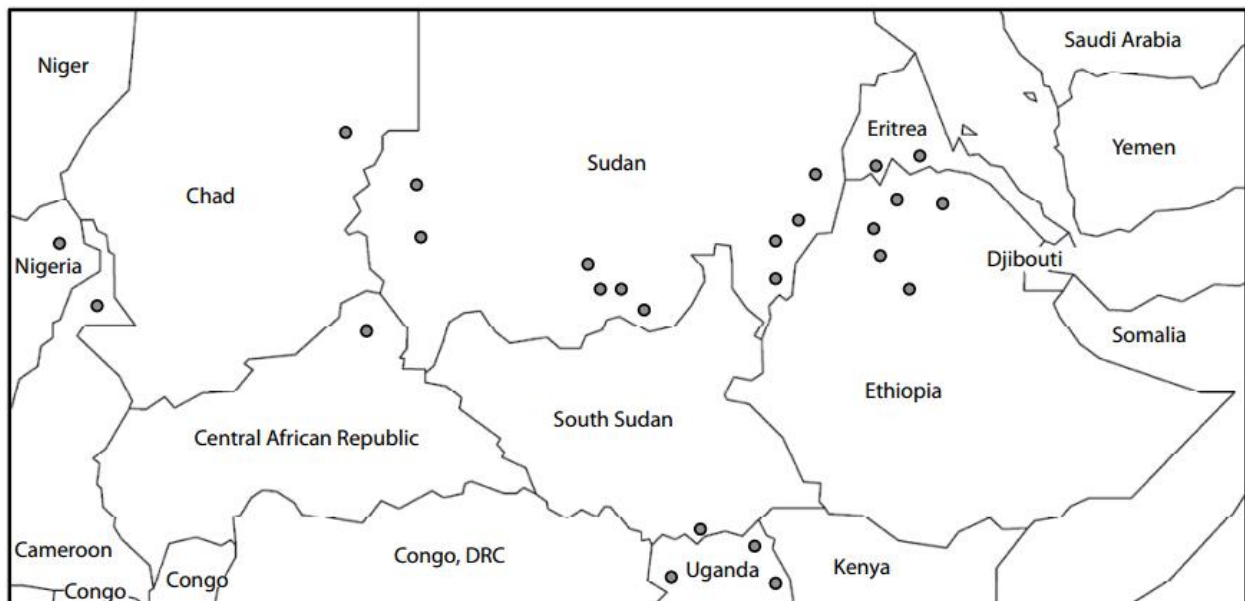
The leaves, bark, root and the resin are also used as traditional medicines for curing various diseases [50, 51]. As it is the source of frankincense (gum olibanum) tapped for cash income and local uses. The major use of the species is the production of frankincense or “olibanum” by tapping the stem [52] and in the Horn of Africa it has an important application in local communities for medicinal uses and during religious and coffee ceremonies [53].

1.4.1. Description of the genus

Boswellia papyrifera (Del.) Hochst belongs to the family Burseraceae, which contains up to 600 species in 17 genera [54]. The genus *Boswellia* is spread in the arid regions of African main land extending from Côte d'Ivoire to north-eastern Tanzania. Its distribution extends further in northern Madagascar and in India. North-eastern tropical Africa is centre of diversity for this species [55] particularly predominating and tapped for gum olibanum in Ethiopia.



Figure 1. A *B. papyrifera* tree (centre), its flowers (upper left), leaves (right), bark with a frankincense tear (lower left) and flaking bark (centre bottom)



Reported occurrence of *Boswellia papyrifera*

Figure 2. The distribution of *B. papyrifera*(Del.) Hochst in Africa

Source: Adapted from Hepper (1969) and Vollesen (1989) [55, 56].



Figure 3. Gum (Frankincense) of *B. papyrifera* after tapping from the plant and sun dried.



Figure 4. Tapped, dried Powder gum (Frankincense) of *B. papyrifera*

1.5. Objectives

1.5.1. The general objective

To sustainably synthesis and characterize gold nanoparticles using olibanum gum obtained from benwellia paprifera through greener approaches.

1.5.2. The specific objectives

- ❖ To synthesis gold nanoparticles (AuNPs) through autoclaving with the olibanum gum of benwellia paprifera
- ❖ To Characterize Synthesized gold nanoparticles (AuNPs) by using UV-Vis spectroscopy, FTIR, XRD, TEM and SEAD.

- ❖ To investigate the antibacterial activity of both gram positive and negative bacteria (*Escherichia coli* (*E. coli*) and *Staphylococcus aureus* (*S. aureus*)) of the newly synthesized AuNPs.
- ❖ To study the stability of the newly synthesized AuNPs in a greener approach.

2. REVIEW OF LITERATURE

Sudip Mohapatra, et al., [57] reported the facile and green synthesis of gold nanoparticles using a novel reducing agent 2,3-dihydroxyfumaric acid (DHFA). In this synthesis, PVP stabilized gold nanoparticles show excellent catalytic activity for controlled and complete aerial oxidation of hydroxybenzyl alcohols to hydroxyl-benzaldehydes. Uncapped gold nanoparticles are ferromagnetic in nature at room temperature.

Prasoon Pal Singh and Chittaranjan Bhakat, [58] presented cost effective and safe technique for the synthesis of Gold nanoparticles by using leaves and bark of *Ficus carica* with aqueous solution of 1mM HAuCl_4 . Based on the report the leaves and bark were found to be a reducing agent as well as capping agent which can rapidly reduces auric ions (Au^+ to Au^0).

Mohanan V. Sujith and Soundarapandian Kannan, [59] have reported the biological synthesis of gold nanoparticles by the reduction of HAuCl_4 by using citrus fruits (*Citrus limon*, *Citrus reticulata* and *Citrus sinensis*) juice extract as the reducing and stabilizing agent. A various shape and size of gold nanoparticles were formed when the ratio of the reactants were altered with respect to 1.0 mM chloroauric acid solution. The gold nanoparticles obtained were characterized by UV–visible spectra, transmission electron microscopy (TEM) and X-ray diffraction (XRD).

TEM studies showed the particles to be of various shapes and sizes and particle size ranges from 15 to 80 nm. Selected-area electron diffraction (SAED) pattern confirmed face centered cubic crystal (fcc) phase and crystallinity of the particles.

Saikat Maity et al., [60] a green synthesis of gold nanoparticles (AuNPs) using aqueous solution of a hetero-polysaccharide, extracted from the gum of *Cochlospermum religiosum* (katira gum), has been developed. The role of hetero-polysaccharide as both reducing and stabilizing agent

was reported. The synthesized AuNPs were characterized by Uv-Vis spectroscopy, HR-TEM, XRD and FT-IR experiments. The surface plasmon resonance (SPR) band of Uv-Vis spectrum around 528 nm confirmed the formation of AuNPs. Transmission electron microscopic analysis showed an average size of AuNPs of 6.9 nm. The fcc crystalline nature of these particles was identified by XRD analysis and SAED pattern. These AuNPs also function as an efficient heterogeneous catalyst in the reduction of 4-nitrophenol (4-NP) to 4-aminophenol (4-AP). The reduction of 4-NP follows pseudo-first-order kinetics with rate constant 2.67102 min.

A. Annamalai et al., [61] has attempted to produce gold nanostructures having unusual physicochemical properties. The synthesis of gold nanoparticles was reported to be eco-friendly and non-toxic (AuNPs) when it is biologically synthesized using the leaf extract of *Euphorbia hirta* L. The synthesis of AuNPs was confirmed by a change in extract color from pale yellow to purple and surface plasmon resonance spectra obtained in a range of approximately 530 nm. Nanoparticles whose sizes ranged from 6 nm to 71 nm, were synthesized. Different instrumental techniques were used to characterize the synthesized AuNPs, such as TEM, XRD, EDAX, AFM, particle size analyzer, FTIR and Raman spectra. Also the antibacterial activity of the green synthesized AuNPs against bacterial strains of *Escherichia coli*, *Pseudomonas aeruginosa* and *Klebsiella pneumonia* was studied using MIC method, and found to be highly effective.

Prema. P and Thangapandiyan. S, [62] have presented research attempt to investigate the bactericidal efficacy of gold nanoparticles (AuNPs) on human pathogens. AuNPs were first synthesized by chemical reduction method with Tetrachloroauric acid ($\text{HAuCl}_4 \cdot 3\text{H}_2\text{O}$) as a metal precursor. Characterization of freshly prepared gold nanoparticles was made using X-ray diffractogram (XRD) and scanning electron microscopy (SEM). Average size of the particles ranged from 8.78-21.96 nm. The synthesized AuNPs were found to be spherical in nature. Antibacterial activities of the synthesized Au nanoparticles were assessed by agar well diffusion method. The stabilized AuNPs exhibited excellent antibacterial sensitivity (30mm) to *E. coli*, *K. pneumoniae* and *V. vulnificus* than the other experimental strains used. In this study, it is also concluded that Au nanoparticles with and without stabilizers could act as an effective antibacterial agent and prove as an alternative for the development of new antibacterial drugs to combat resistance problem.

The bacterial action of gentamicin and that of a mixture of gentamicin and 15-nm colloidal-gold particles on *Escherichia coli* K12 examined by the agar-well-diffusion method, enumeration of colony-forming units, and turbidimetry has also been successfully performed by G. L. Burygin et al., [63].

Ameer Azam et al., [64] reported a simple one step microwave irradiation method for the synthesis of gold nanoparticles using Citric acid and CTAB as reducing agent. The expedition reaction is completed under microwave irradiation in short duration and can be applied to generation of spherical gold nanoparticles. The process was characterized using UV-VIS absorption spectroscopy which revealed the formation of gold nanoparticles with surface Plasmon absorption maxima at 590 and 560 nm for 40 and 70 seconds respectively. Morphology and average size of nanoparticles were estimated using AFM and TEM and thus spherical gold nanoparticles in the size range 1-22 nm are observed. Raman Spectra of the sample revealed peaks at 1197 cm^{-1} and 1373 cm^{-1} which confirms the formation of gold nanoparticles. Antibacterial activity of gold nanoparticles as a function of particles concentration against gram negative bacterium *Escherichia coli* was carried out in solid growth media. Antibacterial properties of gold nanoparticles are attributed to their total surface area, as a larger surface to volume ratio of nanoparticles and it provides a more efficient means for enhanced antibacterial activity. Gold nanoparticles show high antimicrobial and antibacterial activity with zone of inhibition of about 22 mm.

Yan Liu et al., [65] casein micelle stabilized sub-10 nm gold nanoparticles (AuNPs) with hydrophilic and biocompatible, were synthesized in aqueous medium by chemical reduction of HAuCl_4 in the presence of amphiphilic protein aggregates, casein micelles. The prepared AuNPs were evidenced by Uv-Vis spectroscopy, TEM, FTIR, and XRD analysis. The size of the AuNPs can be controlled easily by adjusting casein concentration and the environment pH in the system. Furthermore, casein micelle stabilized AuNPs function as effective catalyst to activate the reduction of 4-nitrophenol (to form 4-aminophenol) in the presence of NaBH_4 . The catalytic activity of AuNPs depends upon the nanoparticle size, the casein concentration and the pH used for synthesis. On the basis of their excellent colloidal stability and catalytic function, and biocompatible surface, the casein micelle-stabilized AuNPs hold great promise for being used in nanoscience and biomedical applications.

S. Vijaya Kumar and S. Ganesan, [66] biocompatible gold nanoparticles have gained considerable attention in recent years for potential applications in bio-diagnostics, gas sensing, catalysis, and nanomedicine due to their interesting size-dependent properties. In the present work a chemical reduction method is used to produce gold nanoparticles with different capping agents. These nanoparticles were prepared by reducing HAuCl_4 using citrate and triethanolamine phosphine (THPAL) and then capping with citrate, starch, and gum arabic.

This article describes a general method for the preparation of citrate-, starch-, and gum arabic-coated gold nanoparticles. Non-toxic, water-soluble THPAL was used as a reducing agent in this process. The gold nanoparticles were characterized by ultraviolet-visible (UV-Vis) spectroscopy and transmission electron microscopy.

Chien-Chen Wu and Dong-Hwang Chen, [67] a novel magnetically recoverable Au nanocatalyst was fabricated by spontaneous green synthesis of Au nanoparticles on the surface of gum arabic-modified Fe_3O_4 nanoparticles. A layer of Au nanoparticles with thickness of about 2 nm was deposited on the surface of gum arabic-modified Fe_3O_4 nanoparticles, because gum arabic acted as a reducing agent and a stabilizing agent simultaneously. The resultant magnetically recoverable Au nanocatalyst exhibited good catalytic activity for the reduction of 4-nitrophenol with sodium borohydride. The rate constants evaluated in terms of pseudo-first-order kinetic model increased with increase in the amount of Au nanocatalyst or decrease in the initial concentration of 4-nitrophenol. The kinetic data suggested that this catalytic reaction was diffusion-controlled, owing to the presence of gum arabic layer. In addition, this nanocatalyst exhibited good stability. Its activity had no significant decrease after five recycles. This work is useful for the development and application of magnetically recoverable Au nanocatalyst on the basis of green chemistry principles.

Yan Cui et al., [68] this work examines the molecular mechanism of action of a class of bactericidal gold nanoparticles (NPs) which show potent antibacterial activities against multidrug-resistant Gram-negative bacteria by transcriptomic and proteomic approaches. Gold NPs exert their antibacterial activities mainly by two ways: one is to collapse membrane potential, inhibiting ATPase activities to decrease the ATP level; the other is to inhibit the subunit of ribosome from binding tRNA. Gold NPs enhance chemotaxis in the early-phase reaction. The action of gold NPs did not include reactive oxygen species (ROS)-related

mechanism, the cause for cellular death induced by most bactericidal antibiotics and nanomaterials. Our investigation would allow the development of antibacterial agents that target the energy-metabolism and transcription of bacteria without triggering the ROS reaction, which may be at the same time harmful for the host when killing bacteria

Keya Layek et al., [69] gold nanoparticles deposited on nanocrystalline magnesium oxide is a very efficient catalyst for the reduction of nitroarenes in aqueous medium at room temperature. Sodium borohydride is used as the source of hydrogen for the reduction of nitro groups. This catalytic system selectively reduces the nitro group even in the presence of other sensitive functional groups under very mild conditions in good to excellent yields without the requirement of any promoters. The reaction kinetics of reduction of 4-nitrophenol to 4-aminophenol has been studied by UV-visible spectrophotometry, and its apparent rate constant has been determined and compared with those of other supported gold catalysts. The spent heterogeneous catalyst is recovered by simple centrifugation, and reused for multiple cycles.

Juncheng Liu et al., [70] have presented a straight forward, economically viable, and “green” approach for the synthesis and stabilization of relatively monodisperse Au nanocrystals with an average diameter of 8.2 nm (standard deviation, SD=2.3 nm) by using nontoxic and renewable biochemical α -D-glucose and by simply adjusting the pH environment in aqueous medium. The α -D-glucose acts both as reducing agent and capping agent for the synthesis and stabilization of Au nanocrystals in the system. The UV/Vis spectroscopy, Fourier transform infrared (FT-IR) spectroscopy, transmission electron microscopy (TEM), electron diffraction (ED), and X-ray diffraction (XRD) techniques were employed to systematically characterize Au nanocrystals synthesized. Additionally, it is shown that these α -D-glucose-stabilized Au nanocrystals function as effective catalyst for the reduction of 4-nitrophenol in the presence of NaBH_4 (otherwise unfeasible if only the strong reducing agent NaBH_4 is employed), which was reflected by the UV/Vis spectra of the catalytic reaction kinetics.

Preeti Dauthal and Mausumi Mukhopadhyay [71] gold nanoparticles (AuNPs) were synthesized at room temperature using *Prunus domestica* (plum) fruit extract as reducing agent. The UV-visible absorption spectrum showed a characteristic optical absorption peak of AuNPs at 543 nm. The X-ray diffraction pattern suggested the formation and crystallinity of AuNPs. Spherical AuNPs synthesized with an average particle size of 20 ± 6 nm were confirmed by

transmission electron microscopy. Fourier transform infrared spectroscopy analysis supported the role of water-soluble polyols and amino acids of plum fruit extract for bioreduction and stabilization of AuNPs. The catalytic activity of AuNPs was investigated for 4-nitrophenol (4-NP) reduction using UV–visible absorption spectroscopy. Biosynthesized AuNPs showed a dose-dependent catalytic activity. Catalytic reduction followed pseudo-first-order kinetics with respect to 4-NP.

3. SCOPE OF THE PRESENT STUDY

Many green syntheses of gold nanoparticles using different natural gums have been reported, however olibanum gum capped gold nanoparticles have not yet been synthesized and studied so far. In this study, AuNPs have been synthesized by reduction of HAuCl_4 using olibanum gum (OG), which acts as both reducing and capping agent in aqueous solvent. The natural abundance of olibanum gum make it available in this local area, nontoxic, economically viable and multifunctional nature of the olibanum gum have prompted us to select this gum for the present study. Antimicrobial activity tests were conducted on bacterial strains of *E. coli* and *S. aureus* to evaluate the efficacy of the newly synthesized gold nanoparticles. Thus, the greener synthesis of AuNPs, characterization and antimicrobial property of olibanum gum capped AuNPs were the main focuses of this study.

4. MATERIALS AND METHODS

Olibanum gum (OG)) grade-1 was purchased from Arada market, Gondar, Ethiopia. Sodium chloride was obtained from S D Fine-chem Limited, Mumbai, India. Hydrochloroauric acid (HAuCl₄) was purchased from Sigma-Aldrich (St. Louis, MO, USA). The test strains, *E. coli* (MTCC 1303) and *S. aureus* (ATCC 25923) were obtained from Biotechnology Laboratories, Gondar, Ethiopia. Yeast extract, tryptophan and bacterial grade agar-agar were obtained from Veterinary Laboratories, Gondar, Ethiopia.

4.1. Synthesis of AuNPs

Glassware was cleaned in a bath of freshly prepared aquaregia solution (HCl:HNO₃ 3:1) and then rinsed thoroughly with H₂O prior to use. Before the preparation of AuNPs, the stock solution of 0.5% (0.5 g) Olibanum gum (OG)) was prepared in double distilled water. The solution was stirred overnight and turned into a homogeneous system. An aqueous solution of HAuCl₄ (1 mL, 1 mM) was mixed with a diluted solution of Olibanum gum (3 mL, varied concentration) and added in a boiling tube. The boiling tube was sealed with aluminum foil and kept in an autoclave. AuNPs are prepared by varying the time of autoclaving at 15 psi pressure and 120 °C temperature. AuNPs are obtained by autoclaving for 10 min at 15 psi pressure and 120 °C temperature varying the concentrations of HAuCL₄ and Olibanum gum. The colorless reaction mixture was converted to the characteristic clear blushing red color after autoclaving. The appearance of color was indicated the formation of AuNPs. The solution of synthesized gold nanoparticles was centrifuged at high speed. The pellet and supernatant liquid were separated. The pellet was again dispersed in double-distilled water.

4.2. Characterization

4.2.1. UV–Visible spectra

In order to confirm the formation of AuNPs, the UV–Visible absorption spectra of the prepared colloidal solution was recorded using a UV–Vis–NIR spectrophotometer (UV-3600, Shimadzu) having a scanning range of 200-700 nm against blank autoclaved gum.

4.2.2. FTIR spectra

FTIR analysis was carried out in order to determine the possible functional groups of olibanum gum, which helps in the reduction and stabilization agent of synthesized nanoparticles. The colloidal solution of AuNPs was first lyophilized and the sample was used for FTIR analysis in the form of a thin transparent pellet with KBr. A pure KBr pellet was used as a background and this was subtracted from the FTIR spectra of the olibanum gum and AuNPs sample. FTIR spectra were recorded with an instrument IR Affinity-1 (Shimadzu) in the scanning range of 650-4000 cm^{-1} .

4.2.3. XRD analysis

The crystallinity of the AuNPs was studied by X-ray diffraction (XRD) measurements of olibanum gum capped AuNPs were carried out on X’pert Pro MRD X-ray diffractometer (De Schakel 18, 5651 GH Eindhoven, Netherlands) operating at 40 kV and a current of 30 mA at a scan rate of 0.388 min^{-1} .

4.2.4. TEM analysis

The morphology and size distribution of the olibanum gum capped AuNPs dispersion was carried out by transmission electron microscopy (TEM) measurement; casting nanoparticle dispersion on carbon-coated copper grids and allowed to dry at room temperature. Measurements were done on TECHNAI G2 F30 S-TWIN instrument (FEI Company, Hillsboro, OR, USA) operated at an accelerated voltage of 200 kV with a lattice resolution of 0.14 nm and point image resolution of 0.20 nm.

4.2.5. Antibacterial property of AuNPs

The disc diffusion method was used to study the antibacterial activity of the eco-friendly synthesized AuNPs. Luria–Bertani (LB) agar medium was prepared by adding yeast extract (0.5 g), tryptophan (1 g), sodium chloride (1 g) and bacterial grade agar (2.5 g) in distilled water (100 mL). Then the agar medium was sterilized by autoclaving at a pressure of 15 psi and 120 °C temperature for 30 min. This medium was transferred to sterilized Petri dishes in a laminar air flow. After solidification of media, overnight cultures of *E. coli* (100 µL) and *S. aureus* (100 µL) were spread separately over the surface of the agar media. Sterile discs were kept on these inoculated plates with the help of sterile forceps. Sample (10 µL) solutions were placed on these discs and were incubated at 37 °C for 24 h in a bacterial incubator. The zone of inhibition (ZOI) that appeared around the disc was measured and recorded as the antibacterial effect of olibanum gum capped AuNPs. Ampicillin was used as a positive control in the experiment. The assays were performed in triplicate.

5. RESULTS AND DISCUSSION

5.1. Uv-Visible spectra

The prepared AuNPs were characterized by UV-visible spectroscopy. UV-visible spectroscopy is one of the most widely used and valuable technique for the observation of NPs synthesis. The obtained AuNPs displayed the characteristic surface plasmon resonance (SPR) band located at 520 nm [72], indicating a good dispersion degree of the AuNPs in aqueous solution. The peak position of AuNPs did not change, which clearly suggest that the particles were well dispersed without aggregation. To optimize the nanoparticle synthesis, the influence of different parameters such as concentration of HAuCl_4 and concentration of olibanum gum was studied. The UV-Vis spectra of AuNPs, prepared by reducing different concentrations of HAuCl_4 with 0.5 % olibanum gum for 10 min of autoclaving at 15 psi pressure and 120°C temperature, were shown in Figure 5. The efficacy of formation of AuNPs increased with increasing concentration of HAuCl_4 due to the enhancement in the oxidation of OH groups by gold ions. This may be attributed to the formation of more of AuNPs with the progress of the reaction, since the intensity of the surface plasmon peak is directly proportional to the density of the AuNPs in solution. Furthermore, the production of nanoparticles with 1mM HAuCl_4 was monitored with various concentrations of olibanum gum (0.1-0.5%) for 10 min of reaction time and respective spectra were represented in Figure 6. It was noticed that the efficacy of nanoparticle synthesis increased with increasing concentration of olibanum gum. Moreover, the effect of autoclave time (2-10 min) at 15 psi pressure and 120°C temperature was studied with olibanum gum at 1% and 1mM HAuCl_4 concentrations respective spectra were produced as shown in Figure 7. It was observed that the formation of AuNPs steadily increased with an increase in the reaction time. The results suggest that the reduction capacity of the olibanum gum

increased with reaction time. As the Autoclave time increases, possibly more and more of hydroxyl groups are being converted to carbonyl groups by air oxidation, which in turn reduce the gold ions.

5.2. FTIR analysis of AuNPs

Figure 8 a and b indicate the FTIR spectra of pure olibanum gum and olibanum gum capped AuNPs, respectively. The major stretching frequencies in the spectrum of olibanum gum are observed at 3418, 2943, 1722, 1606, 1422, 1367, 1252, 1149 and 1067 cm^{-1} [curve (a) of Figure 8], while the olibanum gum capped AuNPs showed characteristic stretching frequencies at 3445, 2939, 1723, 1598, 1432, 1368, 1254, 1140, 1031 cm^{-1} [curve (b) of Figure 8]. The bands observed at 3445 cm^{-1} suggest the -OH group, at 2943 cm^{-1} the asymmetric C-H stretch, at 1722 cm^{-1} the carbonyl stretching vibration, at 1606 cm^{-1} the asymmetric stretch of carboxylate, at 1367 cm^{-1} symmetrical stretch of carboxylate, at 1252 cm^{-1} the presence of acetyl group, at 1149 and 1067 cm^{-1} the C-O stretching vibration of ether and alcohol groups. A shift in the peaks of the FTIR spectrum of olibanum gum capped AuNPs was observed from 3418 to 3445 cm^{-1} , 1606 to 1598 cm^{-1} and the remaining peaks are unchanged suggesting the binding of AuNPs with hydroxyl and carboxylate groups of gum. Based on the band shift in the hydroxyl and carboxyl group, it can be inferred that both hydroxyl and carbonyl groups of gum are involved in the synthesis and stabilization of AuNPs.

5.3. XRD analysis of AuNPs

The XRD technique was used to determine and ascertain the crystal structure of eco-friendly synthesized stable AuNPs. For XRD analysis, the prepared sample was lyophilized and the precipitate obtained was kept under vacuum and used for the analysis. Figure 9 clearly shows

four well-defined characteristic peaks at scattering angles (2θ) of 38.25, 43.95, 64.5, 77.21 respectively, corresponding to the (111), (200), (220), and (311) sets of lattice planes which may be indexed as the band for face-centered cubic (fcc) crystal structure of structure of crystalline metallic gold (JCPDS No. 04-0784). This fact reveals that the synthesized AuNPs are of pure crystalline AuNPs. The strongest reflection was obtained from (111) inferring that (111) is the predominant orientation and the prepared AuNPs are crystalline in nature. The absence of any further crystallographic impurities and peak broadening in XRD spectrum indicates the high purity of nanocrystalline AuNPs. The XRD pattern, thus, clearly shows that the synthesized AuNPs were essentially crystalline. Crystallite size of AuNPs was calculated using the Scherer's formula from the XRD pattern and was found to be around 18.1 nm. The observations from the XRD analysis are in good agreement with the TEM analysis (16 ± 2 nm).

5.4. TEM Analysis of AuNPs

Typical TEM images of sustainable green synthesized AuNPs capped with olibanum gum using 1mM HAuCl₄ and 0.5 %, olibanum gum autoclaved for 15 min. were shown in Figure 10. It was evident from the TEM images of the samples indicate the shape anisotropy and the nanoparticles display an amusing variability of shapes in varying sizes. In addition to nanospheres, some prominent anisotropic nanostructures such as nano hexagonal, triangles and polygonal nano prisms; and abundant uneven shaped nanoparticles were observed. These nanoparticles with poly disperse and average particle size distribution of AuNPs (approximately 15 particles) were counted and then plotted into histograms. Histogram of the particle size distribution of AuNPs (Figure 10) depicts that the average particle size of AuNPs is about 18 nm. The selected area electron diffraction (SAED) pattern (Figure 10) exhibits polycrystalline diffraction rings, indicating that these nanoparticles are highly crystalline in nature. These rings

can be attributed to the diffractions from the (111), (200), (220), and (311) planes of cubic-phase metallic gold.

When the concentration of olibanum gum was increased from 0.1 to 0.5 %, the particle size of the AuNPs formed decreased. These results are similar to the one reported earlier for biosynthesis of AuNPs with sodium alginate, in which the concentration of the olibanum gum increased from 0.1 to 0.5% . The decrease in anisotropy and polydispersity with increase in the concentration of olibanum gum was also evident from the TEM images. It is worth noting that the shape of the particles changed from anisotropic nanostructures to spheres, when the concentration of olibanum gum is increased to 1%. This observation shows that the particle size of the AuNPs can be controlled by varying the concentration of HAuCl_4 , olibanum gum and reaction time. At higher concentration of olibanum gum up to 0.5%, the interaction between ionic gold and function groups on olibanum gum as well as the rate of nanoparticle capping were excellent but at high olibanum gum concentration above 0.5%, the broad particle size distribution might be resulted by the increased intermolecular force of olibanum gum molecules which may hinder the dispersion of AuNPs. Thus, insufficient or excess olibanum gum was unfavorable for the stabilization of AuNPs. In this study, As a result, nanoparticles with mono dispersity were obtained with 0.5 % olibanum gum and 15 min of reaction time at 1mM of HAuCl_4 concentration.

5.5. Stability study

Stability of nanoparticles in solution is an important requirement for catalytic and bio medical application. This feature was analyzed by monitoring the SPR under different pH and electrolytic conditions over a reasonable period of time. The bathochromic shift normally observed in UV-visible spectra is an indication of an increase in the size of the particle or

agglomeration of nanoparticles or both. The synthesized nanoparticles did not show any significant change in the intensity or position of the absorbance at 520 nm with increase in the concentration of electrolyte to 1×10^{-2} M (NaCl) (Figure 11A). pH range of 1.2 to 12 did not alter the size of NPs and no major agglomeration was observed (Figure 11B). The olibanum gum capped AuNPs were stable up to six months at room temperature (Figure 11C) due to the capping of olibanum gum. The above observations indicate their stability for catalytic and anti-bacterial applications.

5.6. Microbial Activity

In the present study, the antibacterial activity of olibanum gum capped AuNPs and olibanum gum alone was tested by disc diffusion method using both *E. coli* and *S. aureus* (Figure 12) and the zone of inhibition (ZOI) values for the above mentioned samples were recorded. The details of the antimicrobial experiments were provided in the experimental section. The ZOI appeared around the disc was construed as a measure of the antibacterial effectiveness of olibanum gum capped AuNPs and olibanum gum alone. The diameter of the ZOI of about 19 mm was observed for 5 mg mL⁻¹ of olibanum gum capped AuNPs, where as that of 17 mm was observed for 1 mg mL⁻¹ olibanum gum capped AuNPs for both *E. coli* and *S. aureus*. The negative control i.e., autoclaved pure olibanum gum sample showed no inhibition ability. Based on the results, it was evident that the ZOI decreases with the decrease in concentration of AuNPs (Figure 12) which shows the antibacterial effectiveness of AuNPs. It can also be concluded from the results that the synthesized AuNPs had significant antibacterial activity against both the gram positive and gram negative bacteria i.e., *S. aureus* and *E. coli* respectively.

AuNPs are proved to be highly potent towards antimicrobial activity. The antimicrobial efficiency of AuNPs increases because of their larger total surface area per unit volume [73].

This enhances its biological activity by increasing the contact area of a metal with a microorganism. The antimicrobial activity of green synthesized AuNPs was carried out by disc diffusion method against different pathogenic bacteria of Gram-negative strains of bacteria (*E. coli*) and Gram-positive strains of bacteria (*S. aureus*). The diameter of inhibition values for the above-mentioned samples was recorded. The bacterial inhibition zones of *S. aureus* and *E. coli* were observed around the disc, as shown in Figure 12, while no zone of inhibition was observed for the gum alone. These results revealed that AuNPs synthesized from olibanum gum demonstrated effective antibacterial activity in Gram negative than in Gram-positive bacteria. The present results agree well with the work of other researchers [74]. It can be suggested that Gram-negative strains of bacteria (*E. coli*) with thin cell wall is more susceptible to cell wall damage compared to Gram-positive strain bacteria (*S. aureus*) with a thick cell wall. The mechanism of the antimicrobial effect of AuNPs is still not well understood. Based on this observation, it can however be concluded that the synthesized AuNPs showed significant antibacterial action on both the Gram classes of bacteria.

The mechanism of the bactericidal activity of gold (0) and AuNPs remains to be understood. Several studies suggest that gold tend to have a greater affinity to react with phosphorus and sulfur compounds [75, 76]. The cell wall of the bacteria as is well known, contain many sulfur-containing proteins and these might be preferential sites for the AuNPs to act on. On the other hand, AuNPs of size 1-60 nm react with sulfur-containing proteins inside the cell, as well as phosphorus-containing compounds such as DNA in the cell nucleus. In addition, it is also believed that after penetration into the bacterial cell, AuNPs inactivate bacterial enzymes essential for their metabolic activity, generating hydrogen peroxide and causing bacterial cell death [77, 78]. It is also concluded that the detrimental reactions of AuNPs with

DNA leads the latter to lose its ability to replicate any further and cellular proteins become inactivated on gold ion treatment. Higher concentrations of Au^+ ions have been shown to interact with cytoplasmic components and nucleic acids and affect the bacteria in their metabolic processes such as the cell respiration and cell division, finally causing the death of the cell [79].

6. CONCLUSION

Olibanum gum is an efficient and easily available source of gum for the synthesis of AuNPs. The olibanum gum acts both as a reductant and as a stabilizer without addition of any reducing and capping agent, water acts as an eco-friendly solvent in the synthesis process. The synthesized AuNPs were characterized by various techniques. The XRD pattern showed that the synthesized AuNPs were essentially crystalline. FTIR spectra were found to show that both hydroxyl and carbonyl groups of olibanum gum were involved in the synthesis and stabilization of AuNPs. The morphology by TEM showed that the synthesized AuNPs were spherical in shape and crystalline in nature with the average size distribution of 18 ± 2 nm. The synthesized AuNPs showed significant antibacterial action on both the gram classes of bacteria (*E. coli* and *S. aureus*).

7. REFERENCES

- [1]. Kreibig, U. and Vollmer, M., Optical Properties of Metal Clusters, Springer: Berlin, **1995**.
- [2]. Schmid, G., *Clusters and Colloids, From Theory to Applications*; VCH: Weinheim, Germany, **1994**.
- [3]. Ghosh, S. K., Kundu, S., Mandal, M., and Pal, T., Silver and Gold Nanocluster Catalyzed Reduction of Methylene Blue by Arsine in a Micellar Medium, *Langmuir*, **2002**, 18, 8756.
- [4]. Ghosh, S. K., Pal, T., Kundu, S., Nath, S., and Pal, T., Fluorescence quenching of 1-methylaminopyrene near gold nanoparticles: size regime dependence of the small metallic particles, *Chem. Phys. Lett.* **2004**, 395, 366.
- [5]. Ghosh, S. K., Pal, A., Kundu, S., Nath, S., Panigrahi, S. and Pal, T. Kubo gap as a factor governing the emergence of new physicochemical characteristics of the small metallic particulates, *Chem. Phys. Lett.* **2005**, 412, 5.
- [6]. Kubo, R., Structural nanocrystalline materials, *J. Phys. Soc. Jpn.*, **1962**, 17, 975.
- [7]. Jackson, J. D., Classical Electrodynamics, Wiley: New York, **1975**, p 98.
- [8]. Atwater, H. A., The Promise of Plasmonics technology, *Sci. Am.* **2007**, 296, 56.
- [9]. Park, J. H., Lim, Y. T., Park, O.O., Kim, J. K., Yu J. W., Kim Y.C. Chemistry of Materials, **2004**, 16(4), 688.
- [10]. Narayanan, R, M. A. and Sayed-El., Catalysis with transition metal nanoparticles in colloidal solution: nanoparticle shape dependence and stability, *Journal of Physical Chemistry B*, **2005**, 109(26), 12663.
- [11]. Aslan, K., Jian, Z., Lakowicz, J. R., Geddes, C. D., Saccharide sensing using gold and silver nanoparticles a review, *Journal of Fluorescence*, **2004**, 14(4), 391.
- [12]. Riviere, C., Boudghene, F.P., Gazeau, F., Roger, J. and Pons, J.N., Iron oxide nanoparticle-labeled rat smooth muscle cells: cardiac MR imaging for cell graft monitoring and quantitation, *Radiology*, **2005**, 235(3), 959.
- [13]. M. C. Daniel and D. Astruc, Gold nanoparticles: assembly, supramolecular chemistry, quantum-size-related properties, and applications toward biology, catalysis, and nanotechnology, *Chem. Rev.*, **2004**, 104, 293–346.
- [14]. K. Bogunia Kubik and M. Sugisaka, from molecular biotechnology to nanomedicine *BioSystems*, **2002**, 65, 123–138.

- [15]. V. P. Zharov, J. W. Kim, D. T. Curiel and M. Nanomedicine: Nanotechnology, Biology and Medicine Everts, *Nanomed.:Nanotechnol., Biol. Med.*, **2005**, 1, 326–345.
- [16]. H. Y. Lee, Z. Li, K. Chen, A. R. Hsu, C. Xu, J. Xie, S. Sun and X. PET/MRI dual-modality tumor imaging using arginine-glycine-aspartic (RGD)–conjugated radiolabeled iron oxide nanoparticles, *Chen, J. Nucl. Med.*, **2008**, 49, 1371–1379.
- [17]. D. Pissuwan, S. M. Valenzuela and M. B. Cortie, Therapeutic possibilities of plasmonically heated gold nanoparticles, *Trends Biotechnol.*, **2006**, 24, 62–67.
- [18]. N. N. Greenwood and A. Earnshaw, Chemistry of the Elements, 2nd edn, Butterworth-Heinemann, Burlington, MA, **1997**.
- [19]. M. S. Chen and D. W. Goodman, The Structure of Catalytically Active Gold on Titania, *Science*, **2004**, 306, 252–255.
- [20]. M. Valden, X. Lai and D. W. Goodman, Onset of Catalytic Activity of Gold Clusters on Titania with the Appearance of Nonmetallic Properties, *Science*, **1998**, 281, 1647–1650.
- [21]. I. X. Green, W. Tang, M. Neurock and J. T. Yates, Spectroscopic Observation of Dual Catalytic Sites during Oxidation of CO on a Au/TiO₂ Catalyst, *Science*, **2011**, 333, 736–739.
- [22]. W. Cai, T. Gao, H. Hong and J. Sun, Applications of gold nanoparticles in cancer nanotechnology, *Nanotechnol., Sci. Appl.*, **2008**, 1, 17–32.
- [23]. R. A. Sperling, P. R. Gil, F. Zhang, M. Zanella and W. J. Parak, Biological applications of gold nanoparticles, *Chem. Soc. Rev.*, **2008**, 37, 1896–1908.
- [24]. X. Liu, Q. Dai, L. Austin, J. Coutts, G. Knowles, J. Zou, H. Chen and Q. Huo, A One-Step Homogeneous Immunoassay for Cancer Biomarker Detection Using Gold Nanoparticle Probes Coupled with Dynamic Light Scattering, *J. Am. Chem. Soc.*, **2008**, 130, 2780–2782.
- [25]. D. Tang, R. Yuan and Y. Chai, *Biosensor, Bioelectron.*, **2007**, 22, 1116–1120.
- [26]. C. D. Medley, J. E. Smith, Z. Tang, Y. Wu, S. Bamrungsap and W. Tan, Gold Nanoparticle-Based Colorimetric Assay for the Direct Detection of Cancerous Cells *Anal. Chem.*, **2008**, 80, 1067–1072
- [27]. W. L. Tseng, M. F. Huang, Y. F. Huang and H. T. Chang, Open-tubular gas chromatography using capillary coated with octadecylamine-capped gold nanoparticles, *Electrophoresis*, 2005, 26, 3069–75.
- [28]. I. H. El-Sayed, X. Huang and M. A. El-Sayed, Selective laser photo-thermal therapy of

- epithelial carcinoma using anti-EGFR antibody conjugated gold nanoparticles, *Cancer Lett.*, **2006**, 239, 129–135.
- [29]. P. Mukherjee, R. Bhattacharya, N. Bone, Y. K. Lee, C. R. Patra, S. Wang, L. Lu, C. Secreto, P. C. Banerjee, M. J. Yaszemski, N. E. Kay and D. Mukhopadhyay, Potential therapeutic application of gold nanoparticles in B-chronic lymphocytic leukemia (BCLL): enhancing apoptosis, *J. Nanobiotechnol.*, **2007**, 5, 4.
- [30]. Link, S., El-Sayed, M.A. Shape and size dependence of radiative, non-radiative and photothermal properties of gold nanocrystals, *International Reviews in Physical Chemistry*, **2000**, (19) 409-453.
- [31]. Daniel, M. C. and Astruc, D. Gold nanoparticles: assembly, supramolecular chemistry, quantum-size-related properties, and applications toward biology, catalysis, and nanotechnology, *Chemical Reviews* (Washington, DC, United States), **2004**, 04(1), 293.
- [32]. Ellen, E.C., Judith, M., Anand, G., Catherine J.M., Michael D.W. Gold nanoparticles are taken up by human cells but do not cause acute cytotoxicity, *Small*, **2005**, (1), 325-327.
- [33]. Gannon, C., Patra, C., Bhattacharya, R., Mukherjee, P., Curley, S., Intracellular gold nanoparticles enhance non-invasive radiofrequency thermal destruction of human gastrointestinal cancer cells, *Journal of Nanobiotechnology*, **2008**, 6, 2.
- [34]. Shukla, R., Bansal, V., Chaudhary, M., Basu, A., Bhonde R.R., Sastry, M, Biocompatibility of Gold Nanoparticles and Their Endocytotic Fate Inside the Cellular Compartment: A Microscopic Overview *Langmuir*, **2005**, 21, 10644-10654.
- [35]. Mandal, D., Maran, A., Yaszemski, M., Bolander M., Sarkar, G., The preparation and characterization of gold-conjugated polyphenol nanoparticles as a novel delivery system, *Journal of Materials Science: Materials in Medicine*, **2009**, 20, 347-350.
- [36]. Wenfu, Y., Suree, B., Zhengwei, P., Shannon, M.M., Steven, H.o., Sheng, D. Angew and Te Chemie, Gold Nanoparticle-Enhanced and Size-Dependent Generation of Reactive Oxygen Species from Protoporphyrin IX, *International Edition*, **2006**, 45, 3614-3618.

- [37]. Safavi, A., Absalan, G., Bamdad, F. Effect of gold nanoparticle as a novel nanocatalyst on luminal-hydrazine chemiluminescence system and its analytical application, *Analytica Chimica Acta*, **2008**, 610, 243-248.
- [38]. J. A. Dahl, B. L. S. Maddux and J. E. Hutchison, Toward greener nanosynthesis, *Chem. Rev.*, **2007**, 107, 2228–2269.
- [39]. (a) P.-H. Chiu, C.-J. Huang and Y.-H. Wang, Characterization and Synthesis of GSCS Nanoparticles by Sol–Gel Method with Controlling of Adding Water Amount, *J. Electrochem. Soc.*, **2008**, 155, K183–K189;
- (b) Y.-J. Choi, C.-K. Chiu and T.-J. M. Luo, Spontaneous deposition of gold nanoparticle nanocomposite on polymer surfaces through sol–gel chemistry, *Nanotechnology*, **2011**, 22, 045601.
- [40]. (a) C. M. Niemeyer, W. Burger and J. Peplies, Angew. Assembly of Gold Nanoparticles Using Genetically Engineered Polypeptides Chem., Int. Ed., **1998**, 37, 2265-2268; (b) Y. Niu and R. M. Crooks, Dendrimer-encapsulated metal nanoparticles and their applications to catalysis, *Chem. Mater.*, **2003**, 15, 3463–3467.
- [41]. C. J. Murphy, Nanocubes and Nanoboxes, *Science*, **2002**, 298, 2139–2141.
- [42]. J. Liu, G. Qin, P. Raveendran and Y. Ikushima, Facile Green Synthesis, Characterization, and Catalytic Function of b-d-Glucose-Stabilized Au Nanocrystals, *Chem. Eur. J.* **2006**, 12, 2131-2138
- [43]. a) M. Brust. , M. Walker, D. Bethell, D. J. Schiffrin, R. Whyman, Synthesis of Thiol derivatised Gold Nanoparticles in a Two-phase Liquid-Liquid System, *J. Chem. Soc. Chem. Commun.* **1994**, 7, 801.
- [44]. P. T. Anastas, J. C. Warner, Green Chemistry: Theory and Practice, Oxford University Press, New York, **1998**.
- [45]. Lemenih, M. and Teketay, D. Frankincense and myrrh resources of Ethiopia: II. Medicinal and industrial uses. SINET: *Ethiopian Journal of Science*, **2003**, 26: 161–172.
- [46]. White F., The vegetation of Africa: descriptive memoir to accompany the UNESCO/AETFAT/UNSO vegetation map of Africa. UNESCO, Paris, **1983**.
- [47]. Ogbazghi W., The distribution of *Boswellia papyrifera*(Del.) Hochst. in Eritrea. PhD Dissertation, Wageningen University, Netherlands **2001**.
- [48]. Adam AA., Some Aspects of Ecology and Management of *Boswellia papyrifera*(Del) Hochst. In Jebel Marra Area Darfur-Sudan. PhD Dissertation. University of Khartoum,

Sudan **2003**.

- [49]. Gebrehiwot K, Muys B, Haile M, Mitloehner R., Introducing *Boswellia papyrifera* (Del.) Hochst and its nontimber forest product, frankincense. *International Forestry Review*, **2003**, 5: 348-353.
- [50]. Tucker A. O., Frankincense and Myrrh. *Economic Botany*, **1986**, 40: 425-433.
- [51]. Eshete A, Teketay D, Hulten H., The socio-economic importance and status of populations of *Boswellia papyrifera* (Del.) Hochst. in Northern Ethiopia: the case of North Gonder Zone. *Forests, Trees and Livelihoods*, **2005**, 15, 55–74.
- [52]. Coppens JJW Flavors and fragrances of plant origin. Food and Agricultural Organization of the United Nations (FAO). Rome, **1995**.
- [53]. Fichtl, R. and Admasu, A., Honey bee flora of Ethiopia. DED/Margraf, Weikersheim, Germany, **1994**, p 510.
- [54]. Vollesen, K., Burseraceae. In: Hedberg, I. and Edwards, S. (eds) *Flora of Ethiopia*, **1989**, Vol. 3.
- [55]. Hepper, F. N., Arabian and African frankincense trees, *The Journal of Egyptian Archaeology*, **1969**, 55: 66–72.
- [56]. Sudip M., Ramachandran K. K. and Tapas K. M., Green synthesis of catalytic and ferromagnetic gold nanoparticles, *Chemical Physics Letters*, 508, **2011**, 76–79.
- [57]. Prasoon P. S. and Chittaranjan B., Green Synthesis of Gold Nanoparticles and Silver Nanoparticles from Leaves and Bark of *Ficus Carica* for Nanotechnological Applications, *International Journal of Scientific and Research Publications*, **2012**, Vol. 2, Issue 5, 2250-3153.
- [58]. Mohanan V. S. and Soundarapandian K., Green synthesis of gold nanoparticles using Citrus fruits (*Citrus limon*, *Citrus reticulata* and *Citrus sinensis*) aqueous extract and its characterization, *Spectrochimica Acta Part A: Molecular and Biomolecular Spectroscopy*, **2013**, 102, 15–23.
- [59]. Saikat M., Ipsita K. S. and Syed S. I., Green synthesis of gold nanoparticles using gum polysaccharide of *Cochlospermum religiosum* (katira gum) and study of catalytic activity, *Physica E.*, **2012**, 45, 130–134.
- [60]. A. Annamalaia, V.L.P. Christina, D. Sudha, M. Kalpana, P. T. V. Lakshmi, Green synthesis, characterization and antimicrobial activity of AuNPs using *Euphorbia hirta*

- L. leaf extract, *Colloids and Surfaces B: Biointerfaces*, **2013**, 108, 60– 65.
- [61]. Prema. P. and Thangapandiyan S., In-Vitro Antibacterial Activity of Gold Nanoparticles Capped With Polysaccharide Stabilizing Agents, *International Journal of Pharmacy and Pharmaceutical Sciences*, **2013**, Vol 5, Issue 1, 0975-1491.
- [62]. G. L. Burygin, E. B. N. Khlebtsova A. N. Shantirokh, L. A. Dykman, V. A. Bogatyre and N. G. Khlebtsov, On the Enhanced Antibacterial Activity of Antibiotics Mixed with Gold Nanoparticles, *Nanoscale Res Lett.*, **2009**, 4:794–801.
- [63]. Ameer Azam et al., One step synthesis and characterization of gold nanoparticles and their antibacterial activities against E. coli (ATCC 25922 strain), *International Journal of Theoretical & Applied Sciences*, **2009**, 1(2):1-4, ISSN: 0975-1718.
- [64]. Yan Liu, Lili Liu, Min Yuan, Rong Guo, Preparation and characterization of casein-stabilized gold nanoparticles for catalytic applications, *Colloids and Surfaces A: Physicochem. Eng. Aspects*, **2013**, 417, 18-25.
- [65]. S. Vijaya Kumar and S. Ganesan, Preparation and Characterization of Gold Nanoparticles with Different Capping Agents, *International Journal of Green Nanotechnology*, **2011**, 3, 47-55.
- [66]. Chien-Chen Wu and Dong-Hwang Chen, Facile green synthesis of gold nanoparticles with gum arabic as a stabilizing agent and reducing agent, *Gold Bulletin*, **2010**, Volume 43 No 4.
- [67]. Yan Cui et al., The molecular mechanism of action of bactericidal gold nanoparticles on Escherichia coli, *Biomaterials*, **2012**, 33, 2327-2333.
- [68]. Keya Layek et al., Gold nanoparticles stabilized on nanocrystalline magnesium oxide as an active catalyst for reduction of nitroarenes in aqueous medium at room temperature, *Green Chem.*, **2012**, 14, 3164.
- [69]. Juncheng Liu et al., Facile “Green” Synthesis, Characterization, and Catalytic Function of b-d-Glucose-Stabilized Au Nanocrystals, *Chem. Eur. J.* **2006**, 12, 2131-2138.
- [70]. Preeti D. and Mausumi M., Prunus domestica Fruit Extract-Mediated Synthesis of Gold Nanoparticles and Its Catalytic Activity for 4-Nitrophenol Reduction, *Ind. Eng. Chem. Res.*, **2012**, 51, 13014–13020.
- [71]. Martínez, J.A., Chequer, N.L., González, J., Cordova, T.: Alternative methodology for gold nanoparticles diameter characterization using PCA technique and UV-VIS spectrophotometry. *Nanosci. Nanotechnol*, **2013**, doi:10.5923/j.nn.20120206.06.

- [72]. Lokina, S., Narayanan, V., Antimicrobial and anticancer activity of gold nanoparticles synthesized from grapes fruit extract, *Chem. Sci. Trans.*, **2013**, doi:10.7598/cst2013.22
- [73]. El-Batal, A. I., Hashem, A. A. and Abdelbaky, N. M., Gamma radiation mediated green synthesis of gold nanoparticles using fermented soybean-garlic aqueous extract and their antimicrobial activity. *Springerplus*, **2013**, 2, 1–10.
- [74]. D.W. Hatchett, S. Henry, Electrochemistry of sulfur adlayers on low-index faces of silver, *J. Phys. Chem.*, **1996**, 9854-9859.
- [75]. S. Ahrland, J. Chatt, N. R. Davies, The relative affinities of ligand atoms for acceptor molecules and ions, *Q. Rev. Chem. Soc.*, **1958** 12, 265–276.
- [76]. M. Raffi, F. Hussain, T. M. Bhatti, J. I. Akhter, A. Hameed, M.M. Hasan, Antibacterial characterization of silver nanoparticles against E. coli ATCC-15224, *J. Mater. Sci. Technol.*, **2008**, 24, 192–196.
- [77]. G. D. Stockman, J. F. Barrett, Structure, function, and assembly of cell walls of gram-positive bacteria, *Annual Review of Microbiology*, **1983**, 37, 501–527.
- [78]. A. Kumar, P. Kumar-Vemula, P.M. Ajayan, G. John, Silver-nanoparticle embedded antimicrobial paints based on vegetable oil, *Nature Materials*, **2008**, 7, 236–241.
- [79]. Q. L. Feng, J. Wu, G. Q. Chen, F. Z. Cui, T. N. Kim, J. O. Kim, A mechanistic study of the antibacterial effect of silver ions on E. coli and Staphylococcus aureus, *J. Biomed. Mater. Res.*, **2000**, 52, 662–668.

APPENDICES

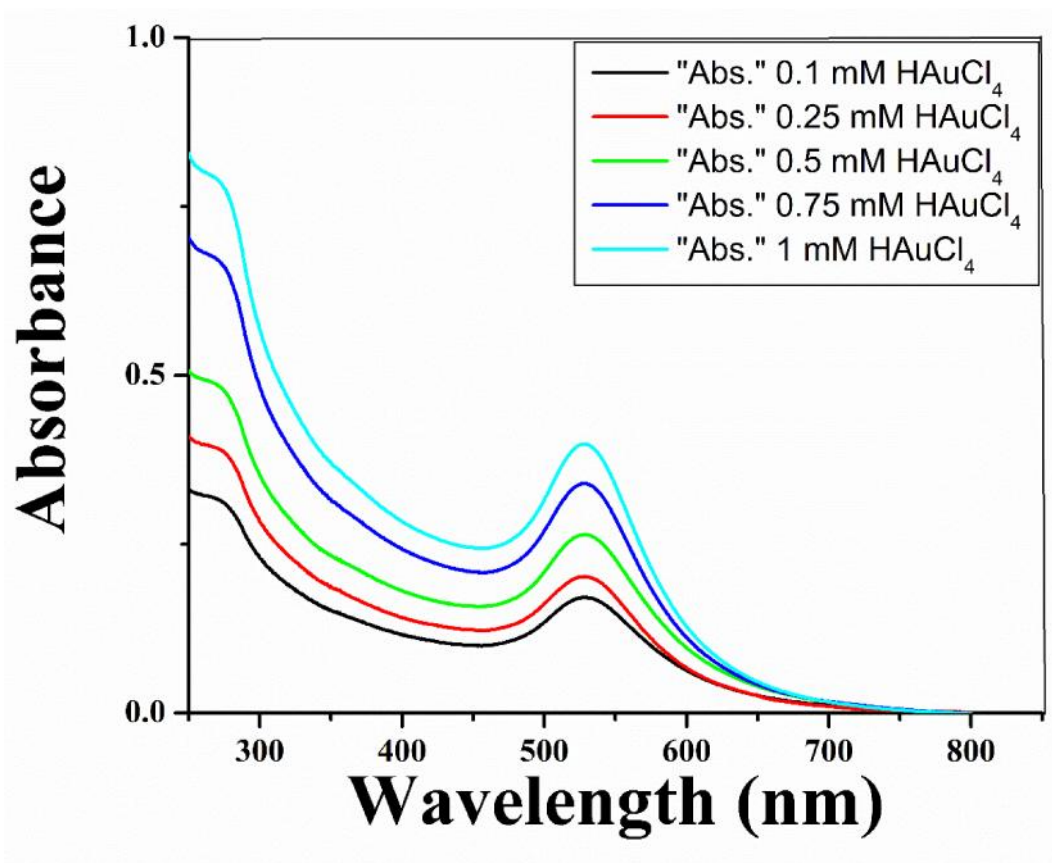


Figure 5. The UV–Vis absorption spectra of AuNPs synthesized by autoclaving different concentrations of HAuCl₄ with 0.5 % olibanum gum solution

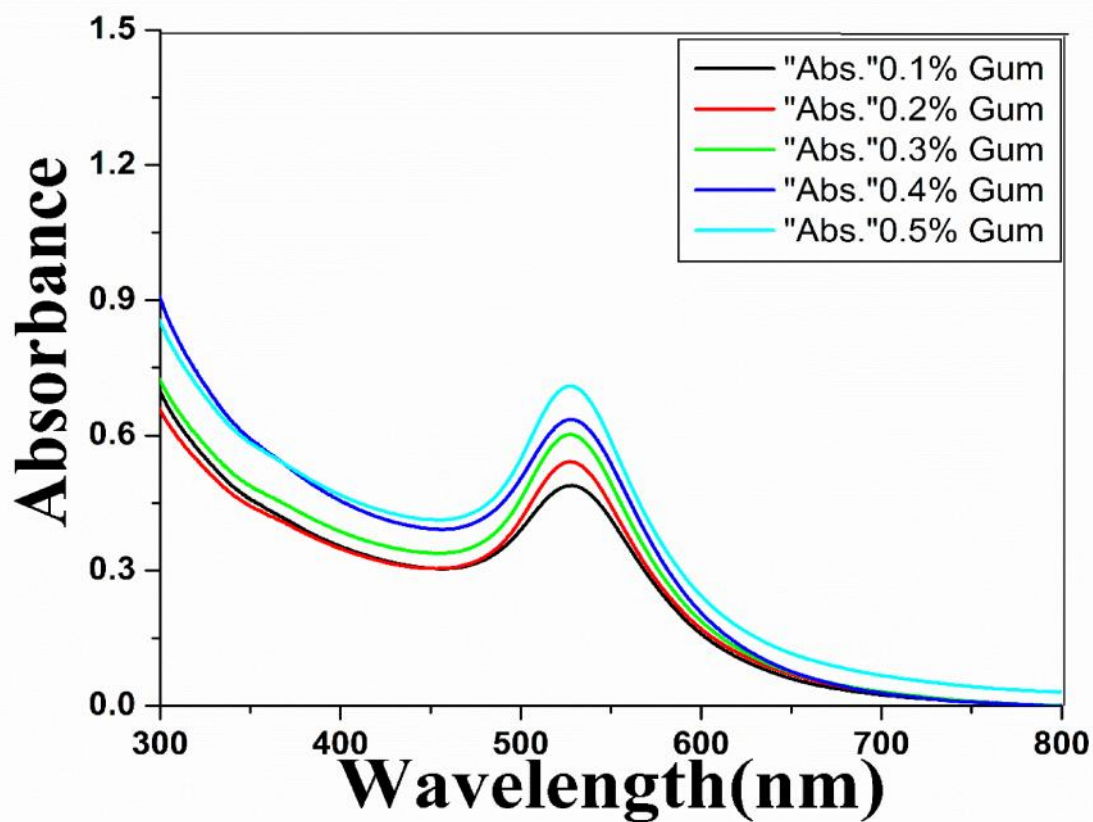


Figure 6. The UV–Vis absorption spectra of AuNPs synthesized by autoclaving different concentrations of olibanum gum solution with 1 mM HAuCl₄

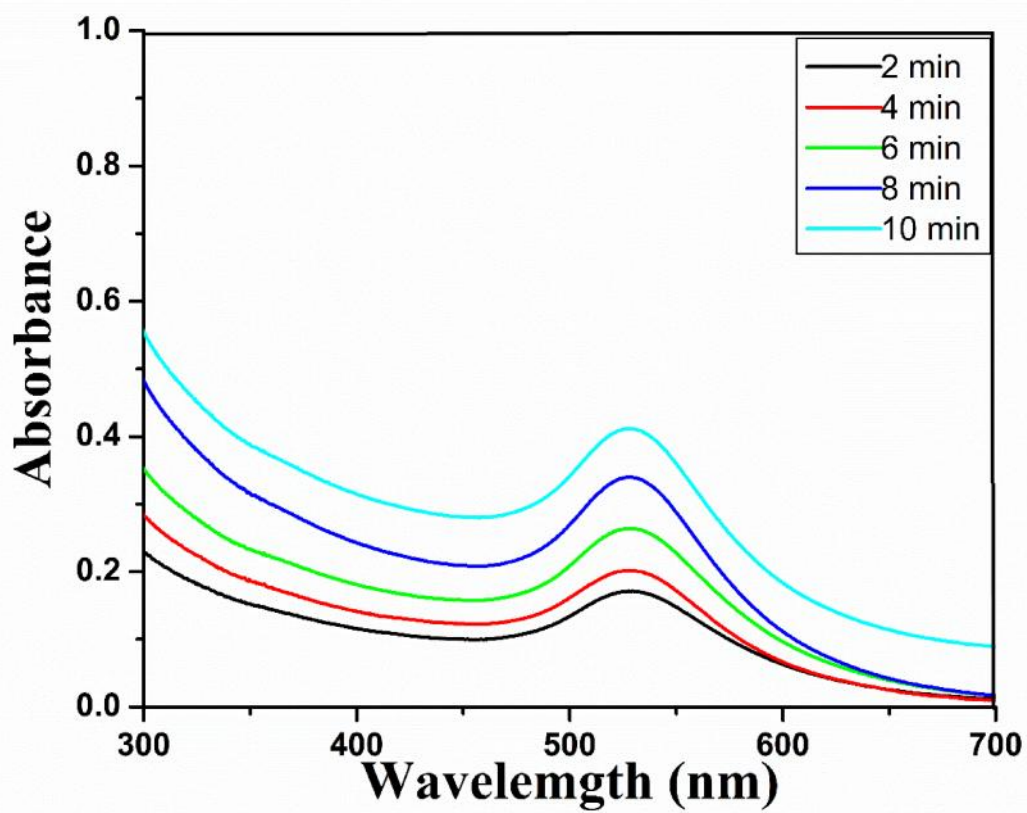


Figure 7. The UV-Vis absorption spectra of synthesized AuNPs by olibanum gum solution with 1 mM HAuCl_4 0.5 % of Olibanum gum solution with different autoclave time.

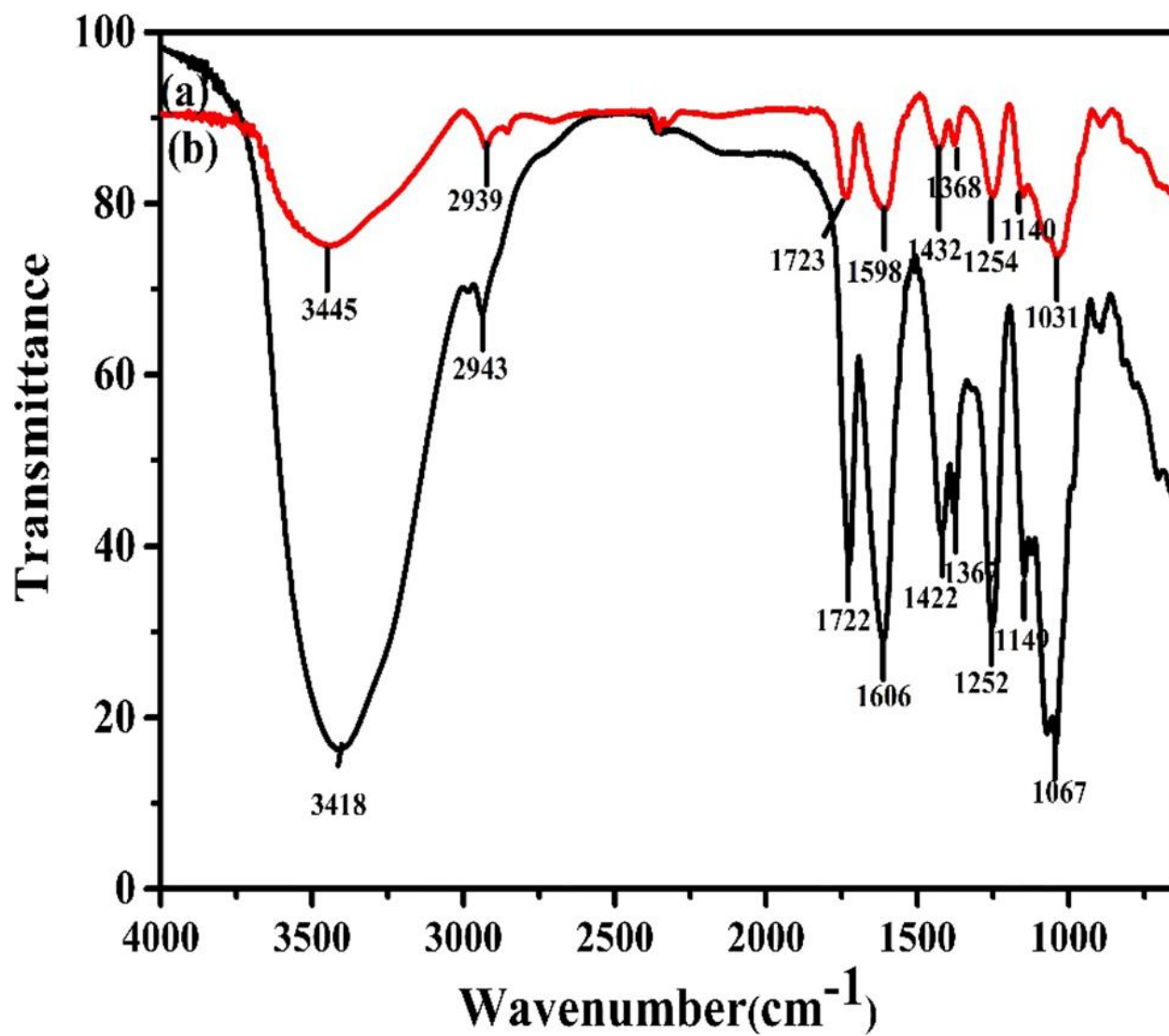


Figure 8. FTIR spectra of (a) olibanum gum, (b) AuNPs capped in olibanum gum

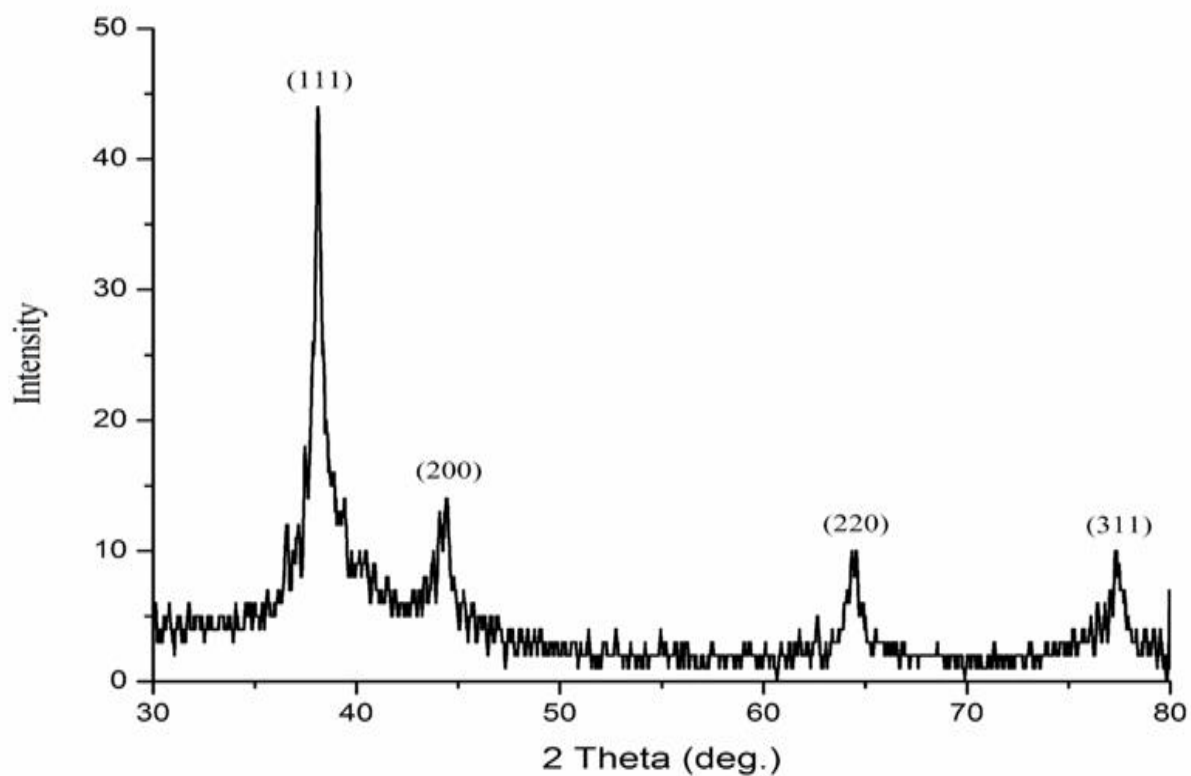


Figure 9. XRD pattern of AuNPs stabilized in olibanum gum. Conditions: 0.5 % (w/v) of gum solution, 1 mM of HAuCl_4 and autoclaved for 15 min at 15 psi.

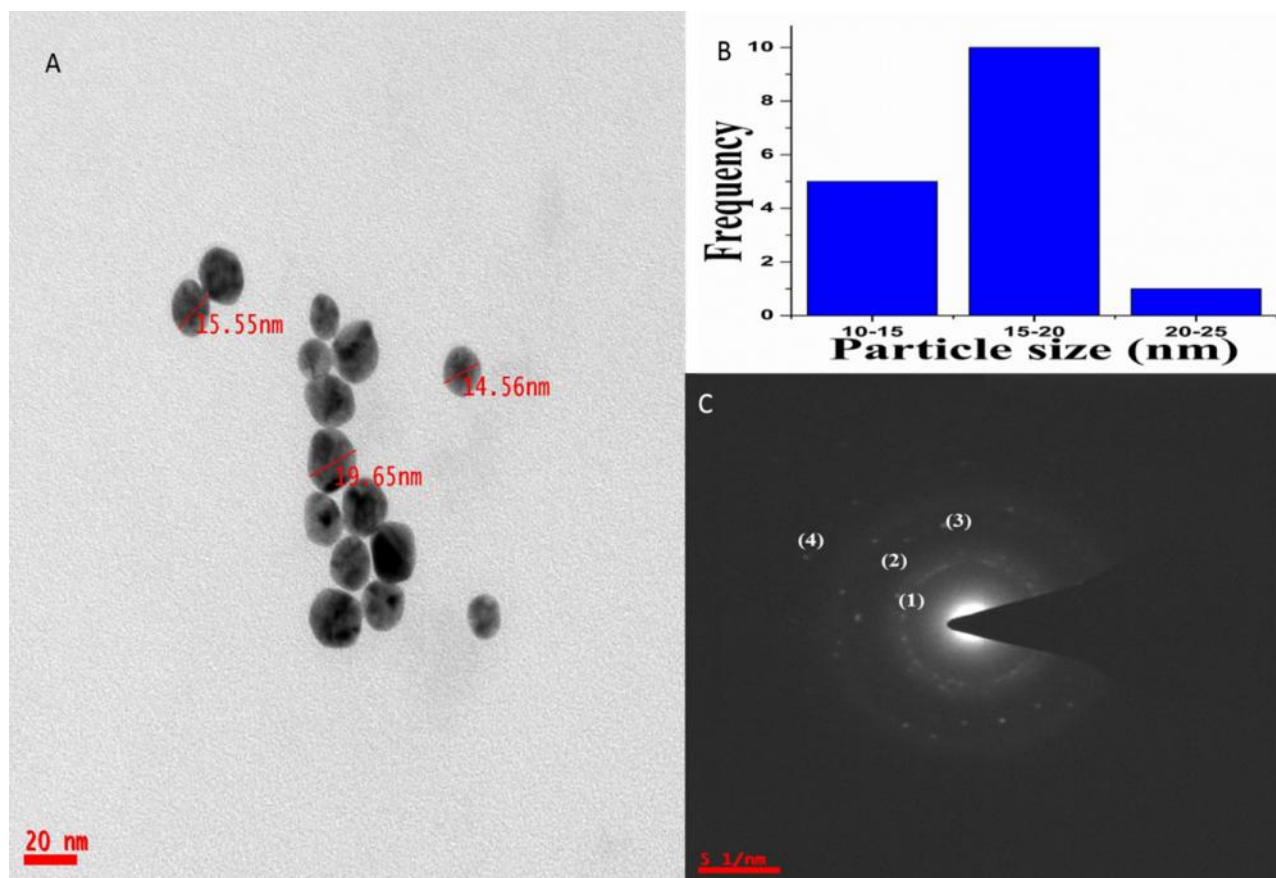


Figure 10. TEM image of gold nanoparticles synthesized with 1 % (w/v) olibanum gum and 1 mM HAuCl_4 , autoclaved for 15 min at 15 psi (B) histogram showing the particle size distribution of AuNPs (C) The selected area electron diffraction pattern of the AuNPs

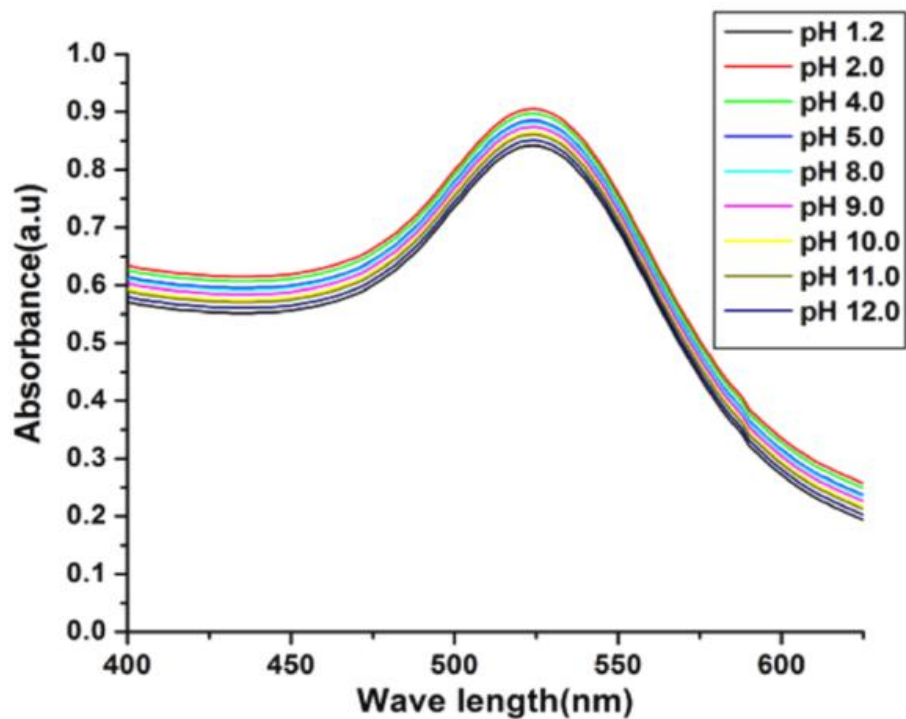


Figure 11A. Stability of gold nanoparticles synthesized with 1 % (w/v) olibanum gum and 1 mM HAuCl_4 , autoclaved for 15 min at 15 psi in different pH condition (pH 2 to 12)

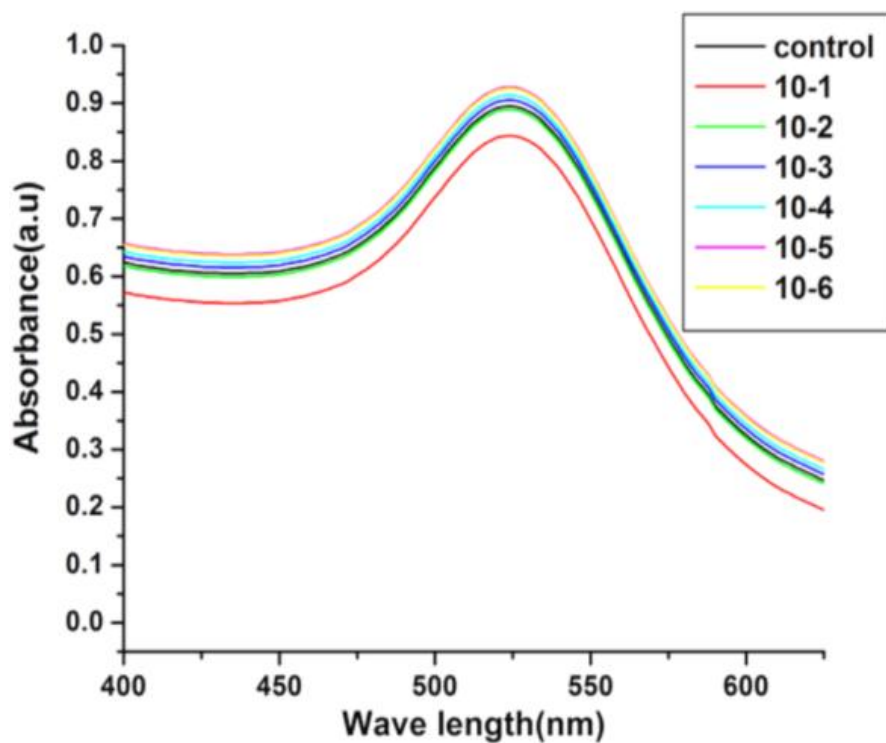


Figure 11B. Stability of gold nanoparticles synthesized with 1 % (w/v) olibanum gum and 1 mM HAuCl_4 , autoclaved for 15 min at 15 psi in different electrolyte condition (10^{-1} to 10^{-6})

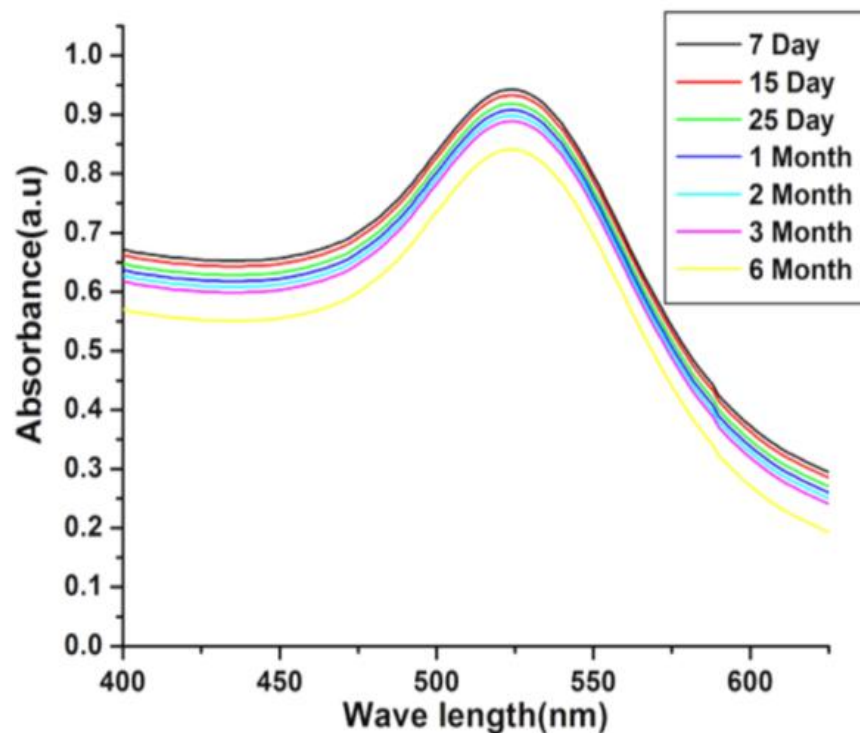


Figure 11C. Stability of gold nanoparticles synthesized with 1 % (w/v) olibanum gum and 1 mMHAuCl₄, autoclaved for 15 min at 15 psi in different days (7 to 1 month)

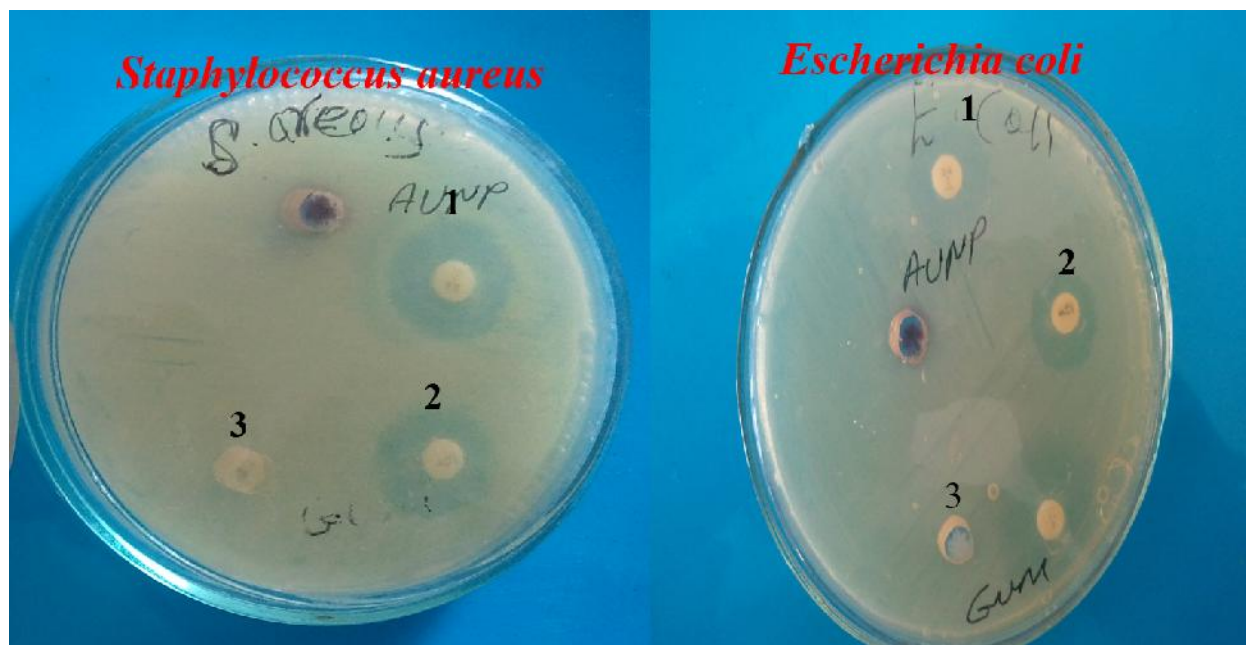


Figure 12. Antibacterial activity of AuNPs against *S. aureus* and *E. coli* after 24 h of incubation. 1. 5 μ L of AuNPs, 2. 5 μ L of ampicillin. 3. 5 μ L of pure olibanum gum solution,